NASA Technical Memorandum 80188

Aerodynamic Characteristics at Low Reynolds Numbers of Several Heat-Exchanger Configurations for Wind-Tunnel Use

William G. Johnson, Jr., and William B. Igoe

DECEMBER 1979

NASA

NASA Technical Memorandum 80188

Aerodynamic Characteristics at Low Reynolds Numbers of Several Heat-Exchanger Configurations for Wind-Tunnel Use

William G. Johnson, Jr., and William B. Igoe
Langley Research Center
Hampton, Virginia

National Aeronautics
and Space Administration

**Scientific and Technical
Information Branch**

1979

SUMMARY

In response to design requirements of the National Transonic Facility, aerodynamic tests were conducted to determine the pressure-drop, flow-uniformity, and turbulence characteristics of various heat-exchanger configurations as a function of Reynolds number. Data were obtained in air with an indraft flow apparatus operated at ambient temperature and pressure. The unit Reynolds number of the tests varied from about 0.06×10^6 to about 1.3×10^6 per meter. The test models were designed to represent segments of full-scale tube bundles and included bundles of round tubes with plate fins in both staggered and inline tube arrays, round tubes with spiral fins, elliptical tubes with plate fins, and an inline grouping of tubes with segmented fins.

Limited analysis of the data from this investigation shows that the downward trend in pressure-drop characteristics as Reynolds number is increased is nominally smooth and well-behaved for most of the configurations. Turbulence data show a relatively homogeneous flow downstream of the heat exchanger with decay occurring as distance from the heat exchanger is increased and show little change with increased Reynolds number. Ranking the configurations in order of pressure-drop and turbulence levels shows that an elliptical-tube plate-fin configuration is the lowest and a round-tube spiral-fin configuration is the highest. The levels of the other configurations tested fall between these two extremes. Flow-uniformity data show that for most inflow conditions on all heat exchangers, the spatial variation in dynamic pressure is less than 20 percent of the average dynamic pressure, which would, in a wind tunnel with a 15 to 1 contraction ratio, result in test-section dynamic-pressure variations of less than 0.1 percent of the average free-stream dynamic pressure. And finally, incoming flow at oblique angles, either parallel to the fins or parallel to the tube axis, did not appreciably degrade the pressure-drop or turbulence characteristics.

INTRODUCTION

The adoption of cryogenic operation has made it possible to achieve high Reynolds number transonic test conditions in conventional pressurized, closed-circuit, fan-driven wind tunnels. The National Transonic Facility (NTF) has been designed to operate at temperatures ranging from ambient to cryogenic with gaseous nitrogen as the test gas and cooling provided by the evaporation of liquid nitrogen directly into the circuit (ref. 1). Additionally, a test capability in air as well as in nitrogen at near-ambient temperatures is provided by using a chilled-water heat exchanger (cooling coil) for temperature control. The Reynolds number range over which the wind tunnel operates in the cryogenic mode usually extends far beyond the range over which the cooling coil is designed for operation in the near-ambient temperature mode. Consequently, it is necessary to determine the aerodynamic characteristics of the cooling coils

throughout this extended Reynolds number range while maintaining as primary design considerations the minimization of pressure loss and turbulence for a given coil heat duty.

An experimental test program was initiated to provide a data base for aerodynamic evaluation of a cooling-coil design. Wind-tunnel tests were made to measure the pressure-drop, flow-uniformity, turbulence, and noise characteristics as a function of Reynolds number for a series of geometric configurations. The program was conducted in two phases. The first phase involved tests in air using an indraft flow apparatus operated at near-ambient temperature and pressure over a range of unit Reynolds numbers from about 0.06×10^6 to about 1.3×10^6 per meter. The second phase involved tests in the Langley 0.3-meter transonic cryogenic tunnel where selected configurations were tested to Reynolds numbers of 28×10^6 per meter. The test models were designed to represent segments of full-scale tube bundles and included bundles of round tubes with plate fins in both staggered and inline tube arrays, round tubes with spiral fins, elliptical tubes with plate fins, and an inline grouping of tubes with segmented fins.

This report presents the results of the first phase of the test program and includes data which show the cooling-coil pressure drop $\Delta p_t/q_\infty$, the three components of turbulence (u'/U, v'/U, and w'/U), and the flow uniformity $\Delta q/q_{avg}$ for the low Reynolds number tests.

SYMBOLS

The measurements of this investigation are presented in the International System of Units (SI) with some U.S. Customary Units indicated in the scales of figures 14 to 21. The measurements and calculations were made in the U.S. Customary Units. Factors relating these two systems of units can be found in reference 2.

Δp_t	total pressure drop across coil model, Pa
q	local dynamic pressure for each probe on survey rake, Pa
q_{avg}	average dynamic pressure measured at survey station using average wall static pressure and average total pressure from the survey rake, Pa
q_∞	free-stream dynamic pressure measured at upstream face of cooling-coil model, Pa
Δq	incremental dynamic pressure for each probe on survey rake, $q - q_{avg}$, Pa
R	unit Reynolds number determined at upstream face of cooling-coil model, per meter
U	mean streamwise velocity

u',v, w' rms values of fluctuating velocity components in streamwise, lateral, and vertical directions, respectively

Abbreviations:

O.C. on-center

O.D. outside diameter

rms root-mean-square

FLOW APPARATUS

A drawing of the flow duct used in the cooling-coil aerodynamic performance tests is shown in figure 1. The indraft flow apparatus operated at near-ambient temperature and pressure. Ambient-condition air was drawn into the bellmouth inlet from the large surrounding room which was vented to maintain constant room air pressure. The tunnel exhausted to the outside of the building. The bellmouth inlet used the coordinates of the ASME long-radius nozzle (ref. 3) attached to a straight duct approximately two inside diameters long. Calibrations of similarly designed inlets showed very flat uniform flow profiles at the end of this combination. A hexagonal cell honeycomb with a 6:1 ratio of cell length to cell width was installed between the bellmouth inlet and transition section to reduce swirl or the effects of ground-vortex entrainment. The transition from the round inlet to the square test section used straight-line elements and was followed by a second 6:1 cell honeycomb and screen installation to further condition the incoming flow. The flow was then introduced to the cooling-coil models through a square duct approximately 1.03 m long. This duct could be adjusted to direct the flow onto the face of the coil model at angles from 90° (normal) to 45° oblique. Downstream of the coil models a square plexiglass duct was used to permit flow visualization. Since the coil models were designed to represent full-scale tube bundles, the downstream duct was made sufficiently long (approximately 2.03 m) to allow flow measurements at locations representative of full-scale distances behind the coil models. The flow was then diffused through a reverse-transition and conical diffuser and left the building through the variable-speed drive fan. Photographs of the flow duct and installed instrumentation are shown in figure 2.

MODEL DESCRIPTION

All the cooling-coil models were designed to represent full-scale tube bundles. Since heat transfer was not included in the aerodynamic tests, it was not necessary to construct the tube bundles of actual tube hardware. Therefore, most of the tube bundles were simulated by using thin flat metal sheets for fins and spacers separating the fins for tubes. The bundles were held together with threaded rods. Only the two tube bundles which did not have plate fins (the spiral-fin tube and segmented-fin tube) were constructed with actual hardware. The model segments were 46.36 cm square, with the streamwise depth of the cooling-coil tube bundle sufficient for simulating a reference heat duty. After testing was completed, it was discovered that the elliptical tube model had

streamwise depth sufficient for only about three-fourths of the reference heat duty. The effect of this modeling deficiency on the test parameters is discussed with the data in the section entitled "Discussion of Results." Drawings and photographs of the various cooling-coil configurations are shown in figures 3 to 8.

TESTS AND MEASUREMENTS

Flow conditions within the test apparatus were established by setting a range of drive-fan rotational speeds up to the maximum allowed for safe fan operation. The resulting Reynolds number based on the speed of the incoming flow at the face of the coil model varied from about 0.06×10^6 to about 1.3×10^6 per meter. For the clear duct the Reynolds number was somewhat higher, ranging from 0.16×10^6 to 1.8×10^6 per meter.

In addition to the normal (90°) incoming flow tests, the cooling coils were also tested with oblique (45°) flows to the face of the coil. The purpose of these additional tests was to assess the effect of the flow near the walls of ducts such as a wide-angle diffuser on the cooling-coil aerodynamic characteristics. In order to obtain data on the coil characteristics with the oblique flow parallel to either the fins or the tube axis (see fig. 9, conditions 90° apart in an actual coil installation), the coil model was rotated the 90° within the same duct structure shown in figure 1. Since the duct walls imposed physical boundaries on the flow immediately downstream of the tube bundles, the modeling of the oblique flow conditions was probably inadequate. However, within this limitation, the oblique flow characteristics were measured but should be used for comparison purposes only.

The primary measurements made during this test were to determine the pressure-drop, flow-uniformity, turbulence, and noise characteristics of the various coil configurations. The location and arrangement of related instrumentation are shown in figure 10. Flow-uniformity and turbulence measurements were made at four downstream stations (fig. 1) to determine any edge effects which might influence measurements at a station (station 5) representing the location of a typical installation of antiturbulence screens.

Pressure drop

The pressure drop across the cooling-coil models was obtained from single-probe stagnation-pressure measurements upstream and downstream of the models, recorded on a differential pressure cell, and time-averaged over 48 readings in order to obtain the value used for the data analysis. The location of the downstream measurement was adjusted for each coil in order to maintain the same distance from the downstream face of each coil. All upstream and downstream measurements were 38.10 cm from the respective coil faces.

Flow uniformity

The flow uniformity was measured at four distances downstream of the model with 65 stagnation pressure tubes in four arms of a cruciform rake which

spanned the 46.36-cm inside width and height of the flow duct. These pressures were measured on mechanically stepped pressure scanners.

Turbulence

The flow turbulence downstream of the coil models was measured using two-component crossed hot-wire probes. The hot wires consisted of 5-micron, platinum-coated, tungsten wire with an effective length-to-diameter ratio of about 250. For the turbulence measurements, the hot wires were operated in a constant-temperature mode. Because of physical limitations in the probe support, the measurements of u' and w' were not made at the same location in the duct cross section as the measurements of u' and v'. (See fig. 10.)

Noise

An attempt was made to determine the noise characteristics of the cooling-coil models. Microphones were installed both in the airstream and flush with the test-section sidewalls, both upstream and downstream of the coil model. The signals were recorded on magnetic tape for off-line analysis. Because of the drive-fan noise, the signal-to-background noise ratio was so low as to obscure the interpretation of the data. Therefore, no noise data are included in this report.

PRESENTATION OF RESULTS

The data are presented in the following figures:

DISCUSSION OF RESULTS

The aerodynamic pressure-drop characteristics of the various cooling-coil configurations are presented in figures 11 to 13 for the flows that are normal, 45° oblique parallel to fins, and 45° oblique parallel to tube axis, respectively. The data are shown in nondimensional form $\Delta p_t/q_\infty$ as a function of the Reynolds number per meter. For all the coil configurations in the three incoming flow conditions, the downward trend in pressure drop as Reynolds number is increased is nominally smooth and well-behaved. Generally, this trend diminishes for most of the configurations and actually reverses for the baseline configuration in normal flow for Reynolds numbers between 0.6×10^6 and 1×10^6. The lower values of $\Delta p_t/q_\infty$ for the oblique-flow cases are not a result of an actual lower loss, but of the higher q_∞ measured in the smaller 45° duct ahead of the coil. (See fig. 1.) If the q_∞ normal to the face of the coil had been used, the coils would exhibit similar pressure-drop values. In general, ranking the coil configurations in order of pressure drop shows the elliptical coil to be the lowest, followed in order by the inline, baseline, staggered, segmented, and spiral configurations. It should be noted, however, that the elliptical-coil model had only three-fourths of the reference heat duty.

As stated earlier, flow-uniformity and turbulence measurements were made at several downstream stations to determine any edge effects on these data. Flow-uniformity data are shown in figure 14 at four downstream survey stations for the staggered-coil configuration in the three incoming flow conditions. The data show the variation of the parameter $\Delta q/q_{avg}$ with probe position in the cross section of the duct. As shown in the horizontal surveys of figures 14(a) and 14(b), there appears to be a growing edge effect. This effect appears in the vertical survey of figure 14(c), which indicates that it rotated with the bundle. Therefore, this effect is attributable to the modeling of the tube bundle, and not to the coil design itself. This effect does not influence the region where measurements were made. (See fig. 10.) Flow-uniformity data $\Delta q/q_{avg}$, taken at the 1.78-m station for the clear duct and six cooling-coil

configurations, are given in figures 15 to 21 as a function of probe location. Generally, the repeatability of the data is within acceptable limits. The values of the flow-uniformity parameter are, for most inflow conditions on all coils, within ±0.20. This level in the settling chamber of a wind tunnel with a contraction ratio of 15 to 1 would result in a desired level of $\Delta q/q_{avg}$ in the test section of less than ±0.001.

The decay of turbulence levels downstream of the staggered cooling-coil configuration is shown in figure 22. All three components of the turbulence are plotted as velocity ratios u'/U, v'/U, and w'/U against Reynolds number. Generally, there is little change in turbulence with increasing R; however, the change in turbulence with downstream distance shows a decay to about one-fifth the original level as the distance changes from 55.88 cm to 177.80 cm. The 45° oblique inflow does little to change these trends. As shown in figure 10 and stated previously, the mounting arrangement for the hot wire resulted in two different locations being used to obtain the three components of turbulence: the side mount yielded u' and v'; the top mount yielded w' and a second u'. A comparison of the two u' values gives some indication of the homogeneity of the flow. These data are shown in figures 23 to 25 for all coil configurations in all inflow conditions as a function of R. The data show general agreement in the variation with Reynolds number for each coil but do not always show agreement in the levels of the turbulence component u' for the two different mounting positions. The relative turbulence levels of the various cooling-coil configurations are presented in figures 26 to 28 for the normal flow, 45° oblique flow parallel to fins, and 45° oblique flow parallel to tube axis, respectively. The three components of turbulence are plotted as the velocity ratios u'/U, v'/U, and w'/U against Reynolds number per meter. In most cases, the level of turbulence is relatively stable as R increases. The elliptical coil generally shows the lowest level of turbulence, followed by the baseline, staggered, inline, segmented, and spiral configurations. Again, it should be noted that the elliptical-coil model had only three-fourths of the reference heat duty.

SUMMARY OF RESULTS

In response to design requirements of the National Transonic Facility, wind-tunnel tests were conducted to determine the pressure-drop, flow-uniformity, and turbulence characteristics of various heat-exchanger (cooling-coil) configurations as a function of Reynolds number. Limited analysis of the data from this investigation indicates the following results:

1. The downward trend in pressure-drop characteristics as Reynolds number is increased is nominally smooth and well-behaved. However, this trend diminishes for most of the configurations and actually reverses for the baseline configuration in normal flow for Reynolds numbers between 0.6×10^6 and 1×10^6.

2. Ranking the coil configurations in order of pressure drop shows the elliptical coil to be the lowest, followed in order by the inline, baseline, staggered, segmented, and spiral configurations. It should be noted, however, that the elliptical-coil model had only three-fourths of the reference heat duty.

3. Flow-uniformity data $\Delta q/q_{avg}$ are, for most inflow conditions on all coils, less than ±0.20. This level in the settling chamber of a wind tunnel with a contraction ratio of 15 to 1 would result in a level of $\Delta q/q_{avg}$ in the test section of less than ±0.001.

4. Turbulence data show a relatively homogeneous flow downstream of the coil with decay occurring as distance from the coil is increased and show little change with increased Reynolds number.

5. Ranking the coil configurations in order of turbulence levels shows the elliptical coil to be the lowest, followed by the baseline, staggered, inline, segmented, and spiral configurations. As previously noted, the elliptical-coil model had only three-fourths of the reference heat duty.

6. Oblique angles of inflow, either parallel to the fins or parallel to the tube axis, did not appreciably degrade the pressure-drop or turbulence characteristics.

Langley Research Center
National Aeronautics and Space Administration
Hampton, VA 23665
December 3, 1979

REFERENCES

1. Howell, Robert R.; and McKinney, Linwood W.: The U.S. 2.5-Meter Cryogenic High Reynolds Number Tunnel. High Reynolds Number Research, Donald D. Baals, ed., NASA CP-2009, 1977, pp. 27-51.

2. Mechtly, E. A.: The International System of Units - Physical Constants and Conversion Factors (Second Revision). NASA SP-7012, 1973.

3. Shoop, Charles F.; and Tuve, George L.: Mechanical Engineering Practice - A Laboratory Reference Text. Fifth ed. McGraw-Hill Book Co., Inc., 1956, p. 240.

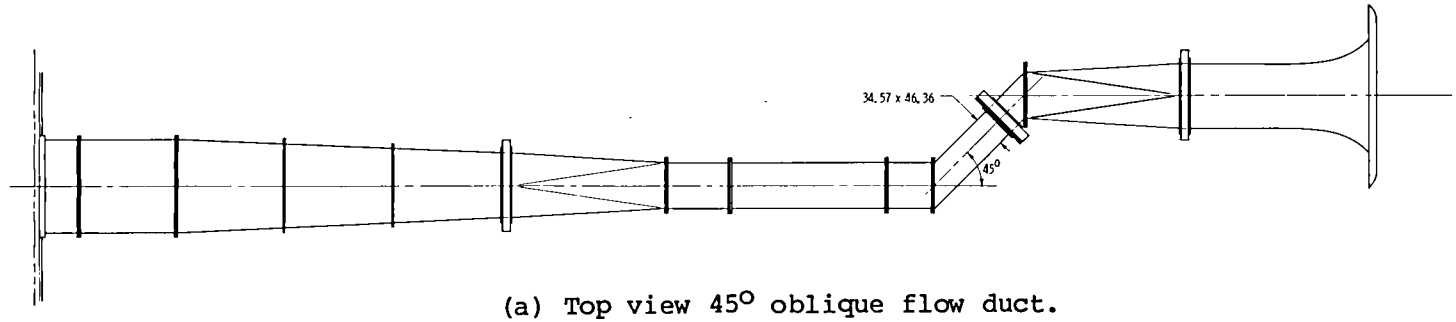

(a) Top view 45° oblique flow duct.

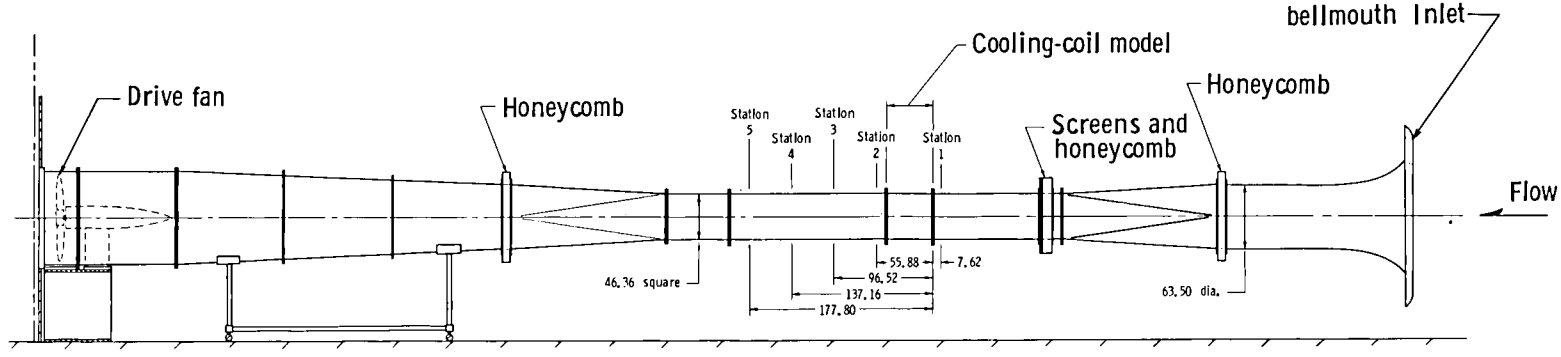

(b) Side view normal flow duct.

Figure 1.- Drawing of flow duct used in cooling-coil performance tests. (All dimensions are in centimeters.)

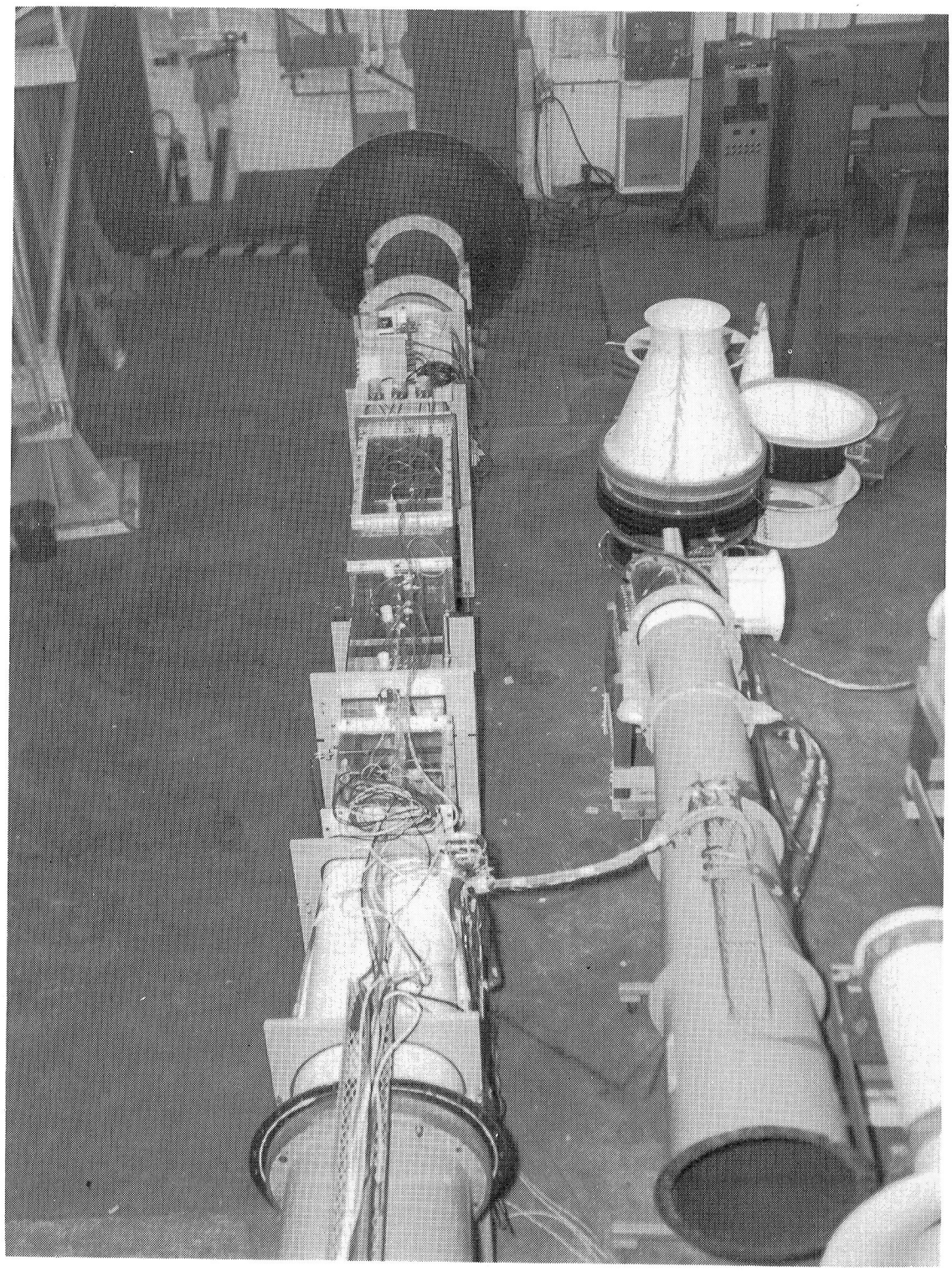

L-76-8267

(a) Normal flow duct assembly.

Figure 2.- Photographs of flow duct used for cooling coil.

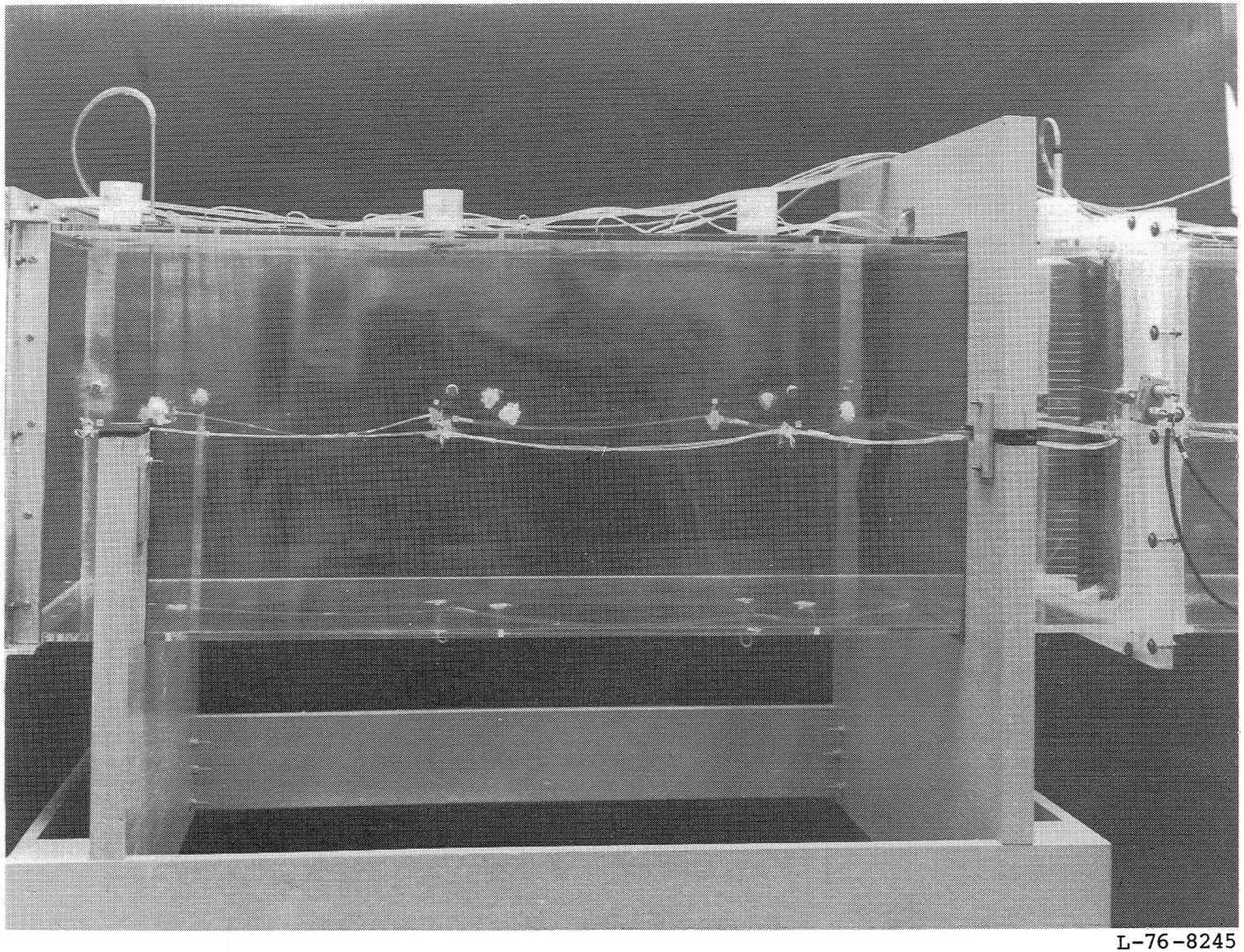

L-76-8245

(b) Downstream survey stations.

Figure 2.- Concluded.

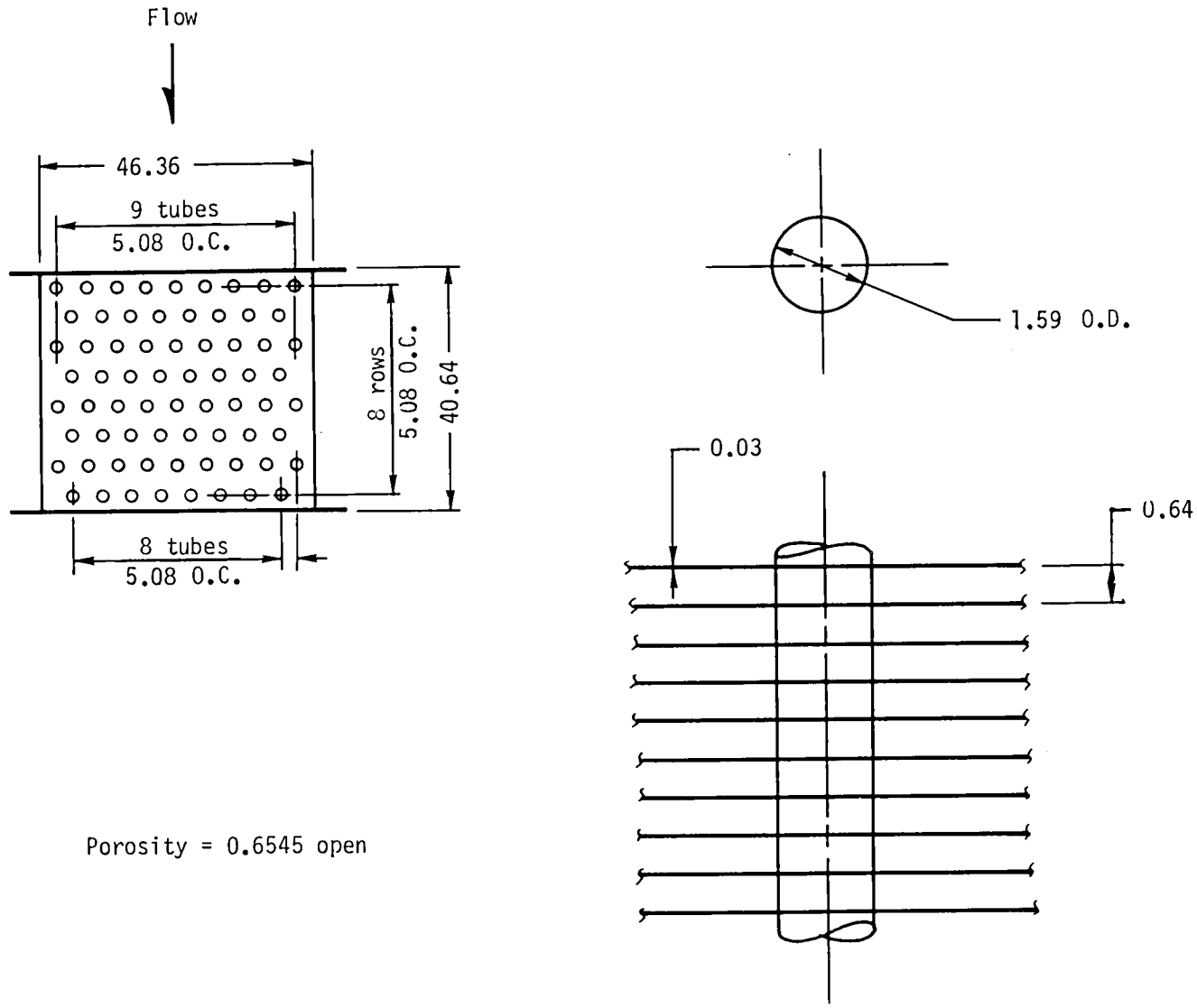

(a) Geometric details.

Figure 3.- Staggered-tube cooling-coil configuration. (All dimensions are in centimeters.)

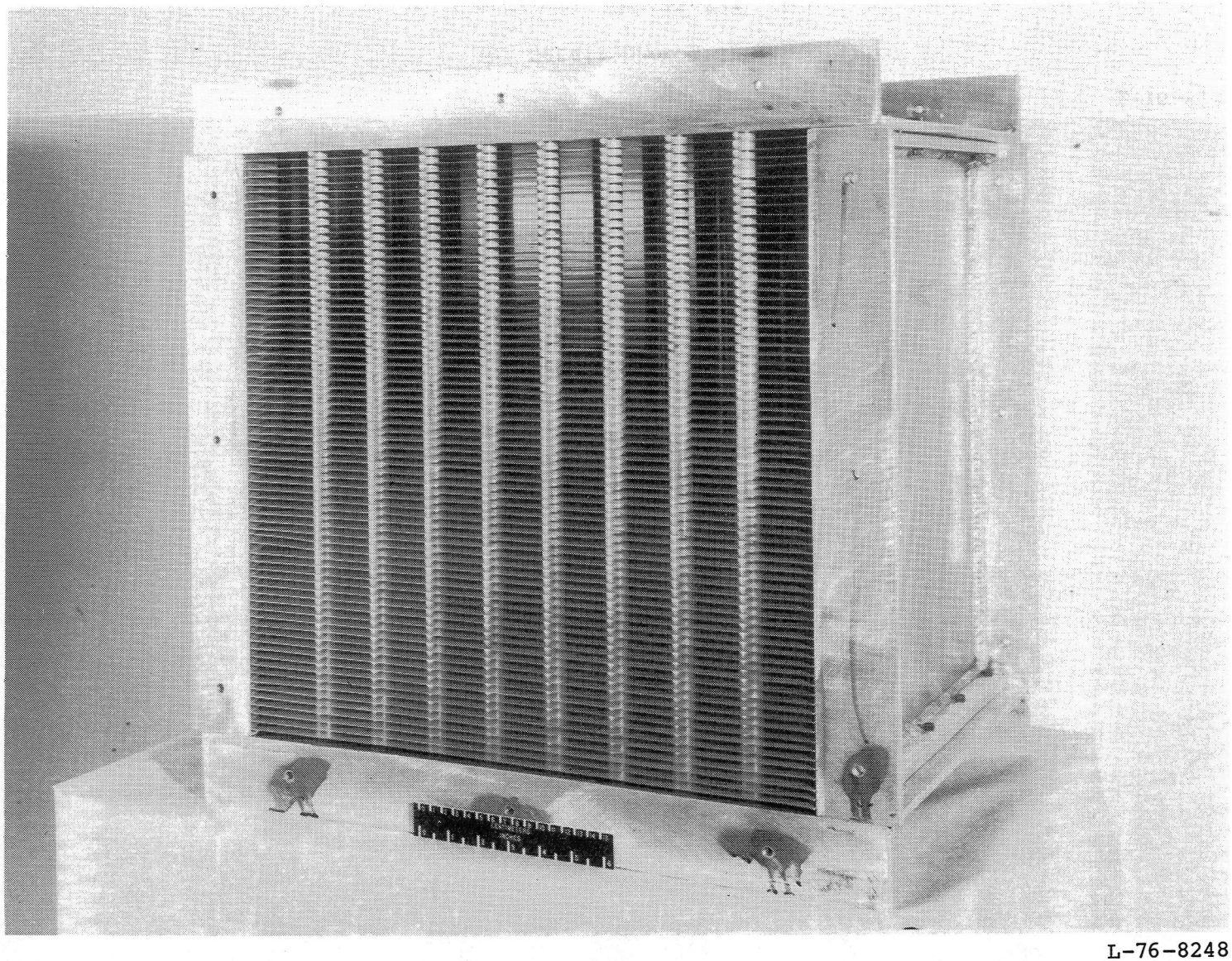

L-76-8248

(b) Photograph of complete tube bundle.

Figure 3.- Continued.

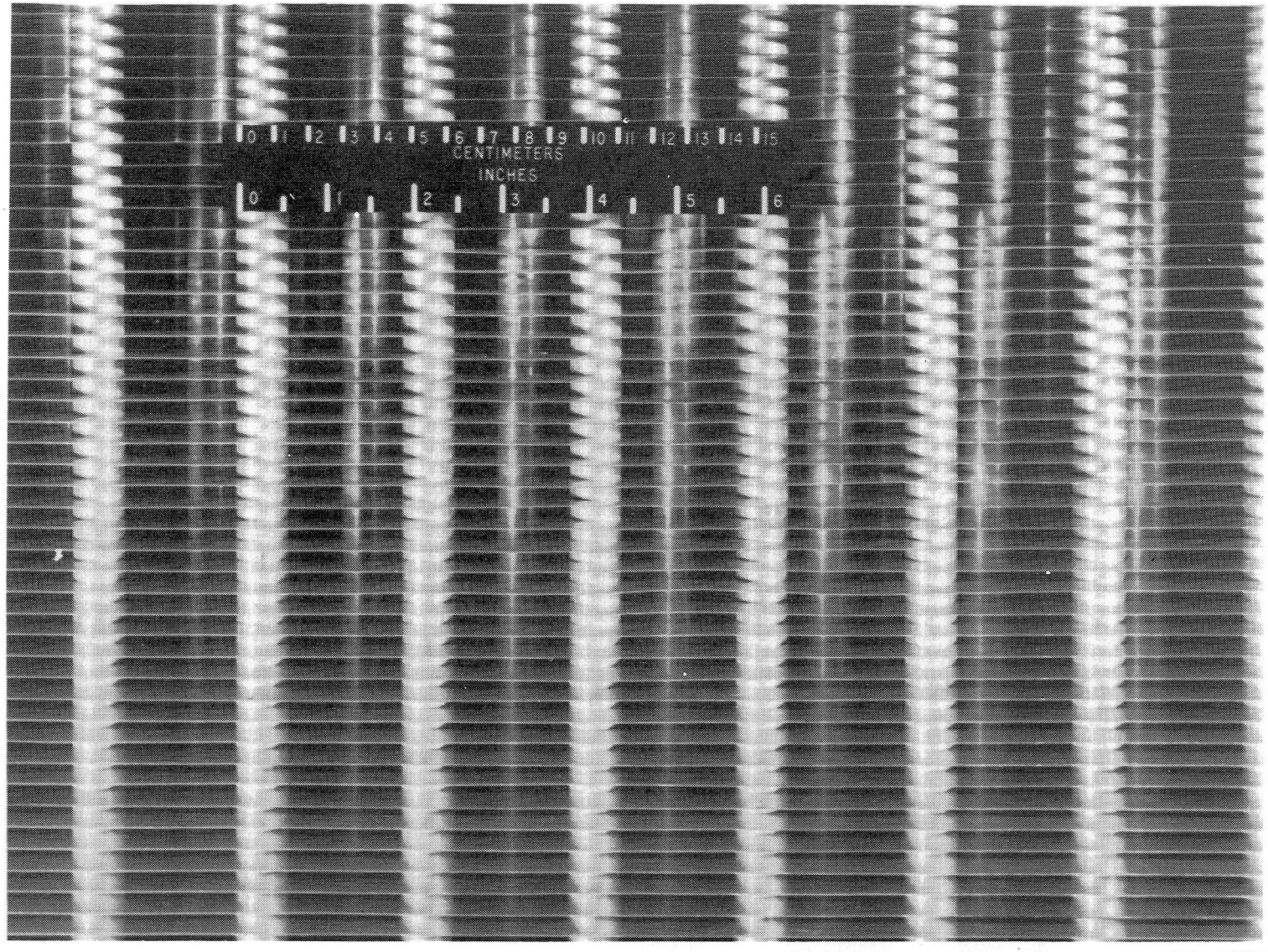

L-76-8239

(c) Detail photograph.

Figure 3.- Concluded.

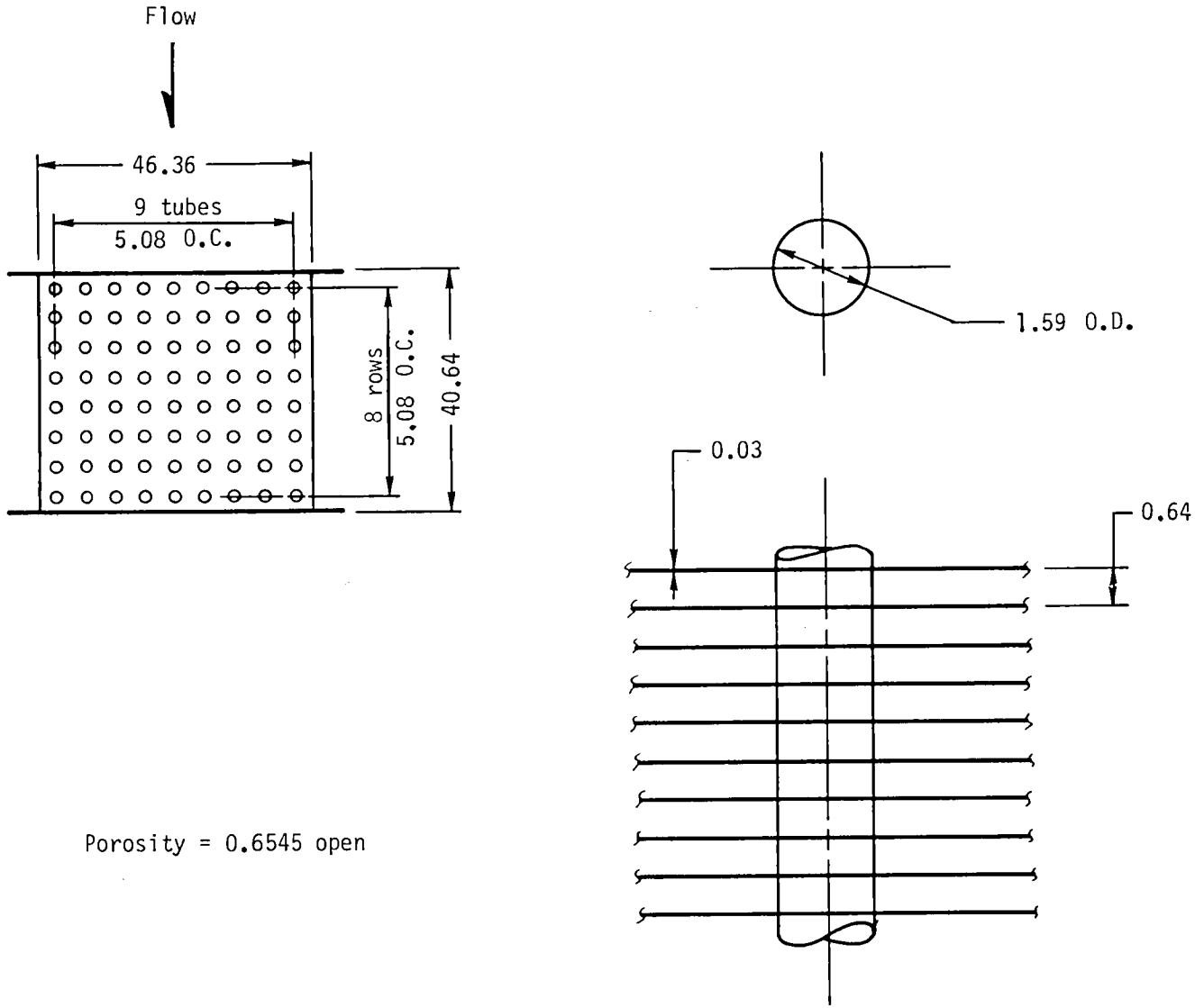

(a) Geometric details.

Figure 4.- Inline-tube cooling-coil configuration. (All dimensions are in centimeters.)

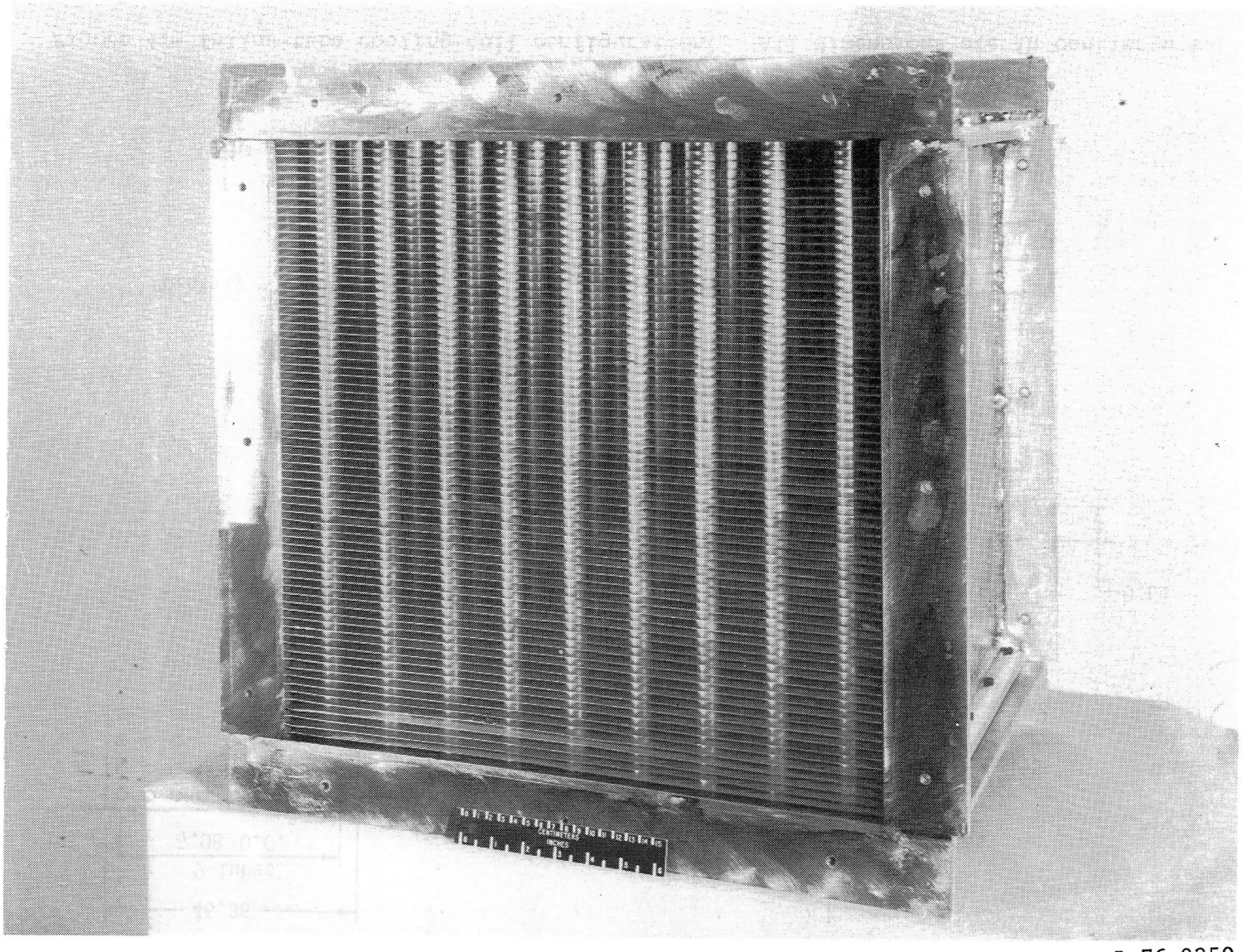

L-76-8250

(b) Photograph of complete tube bundle.

Figure 4.- Continued.

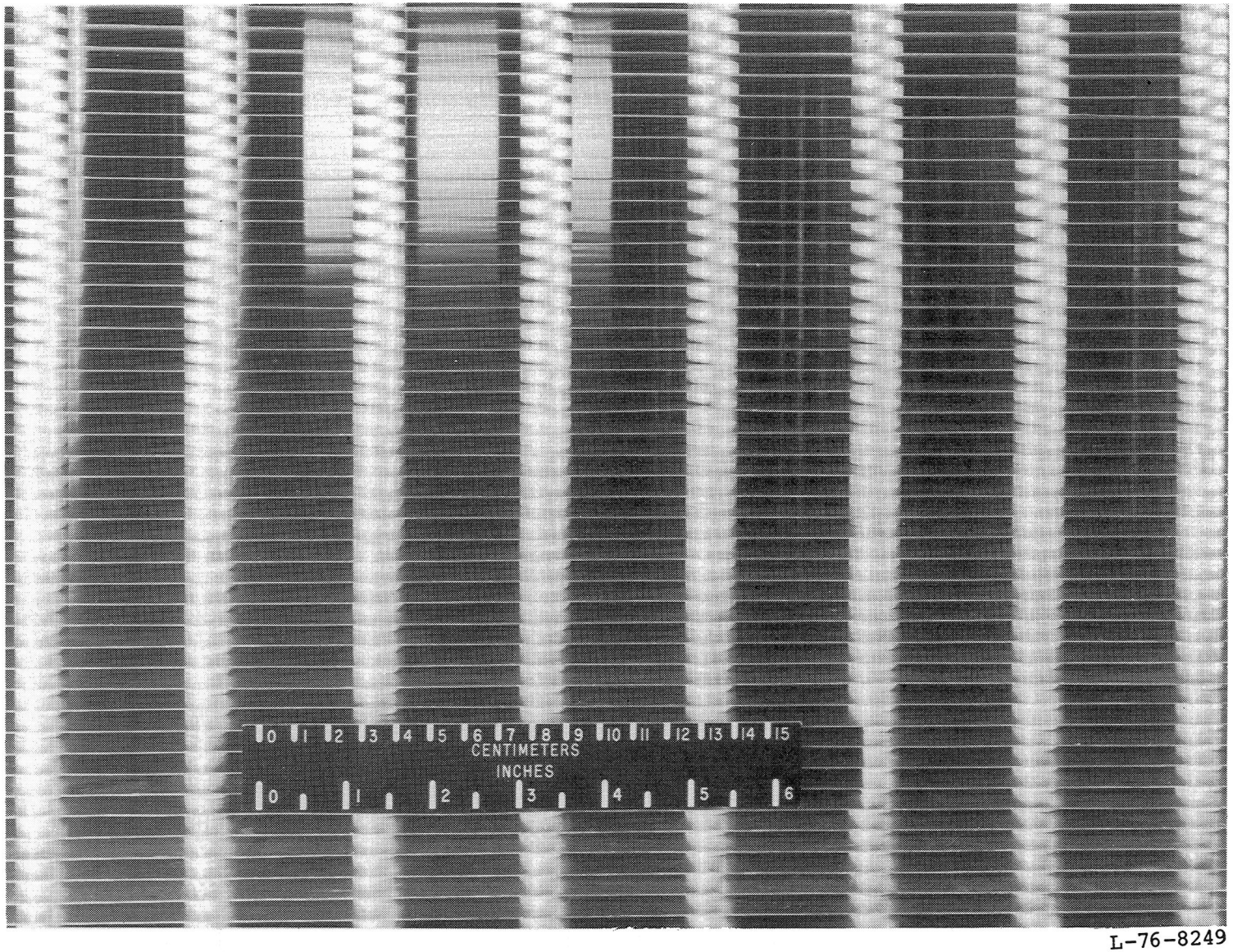

L-76-8249

(c) Detail photograph.

Figure 4.- Concluded.

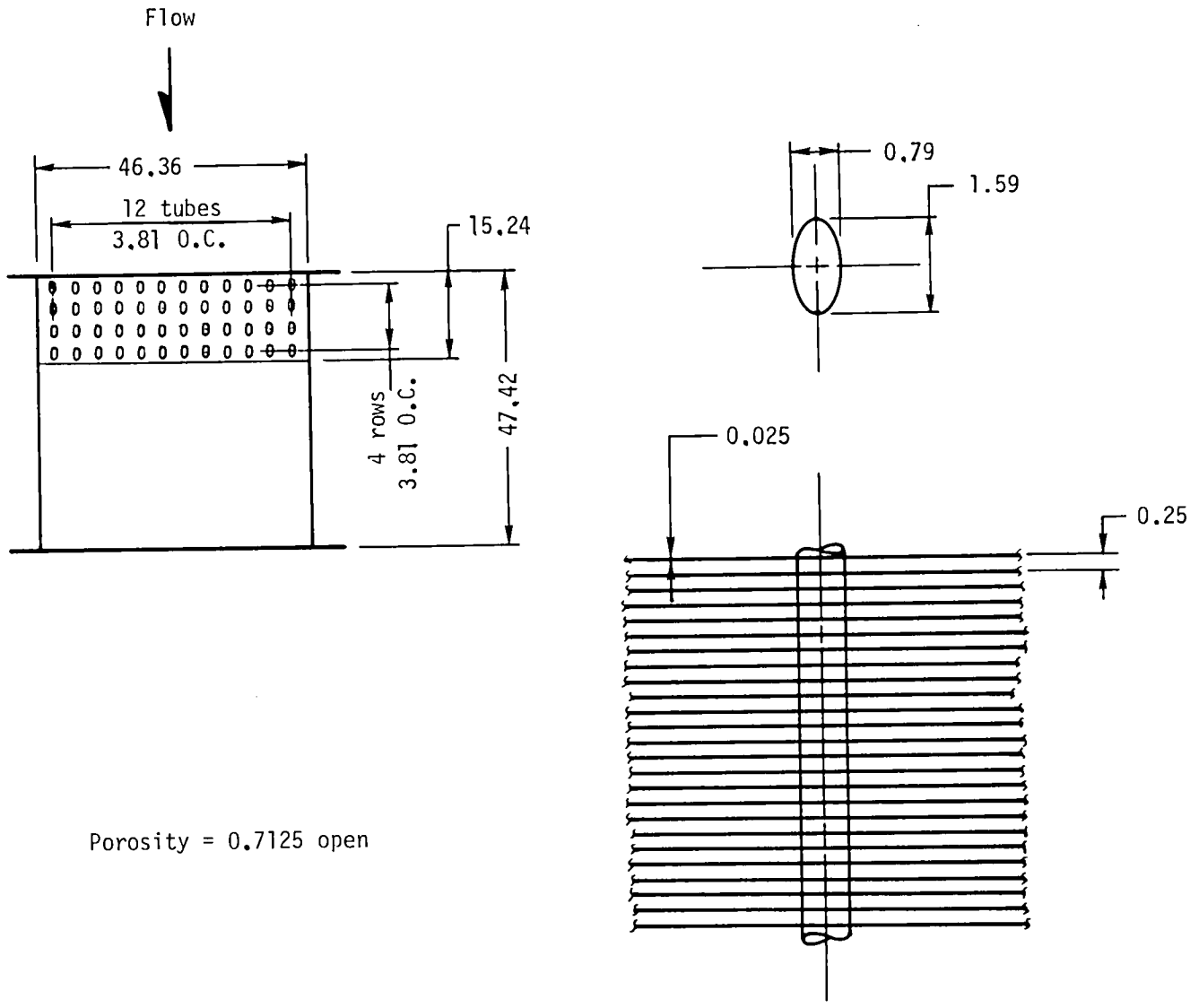

(a) Geometric details.

Figure 5.- Elliptical-tube cooling-coil configuration. (All dimensions are in centimeters.)

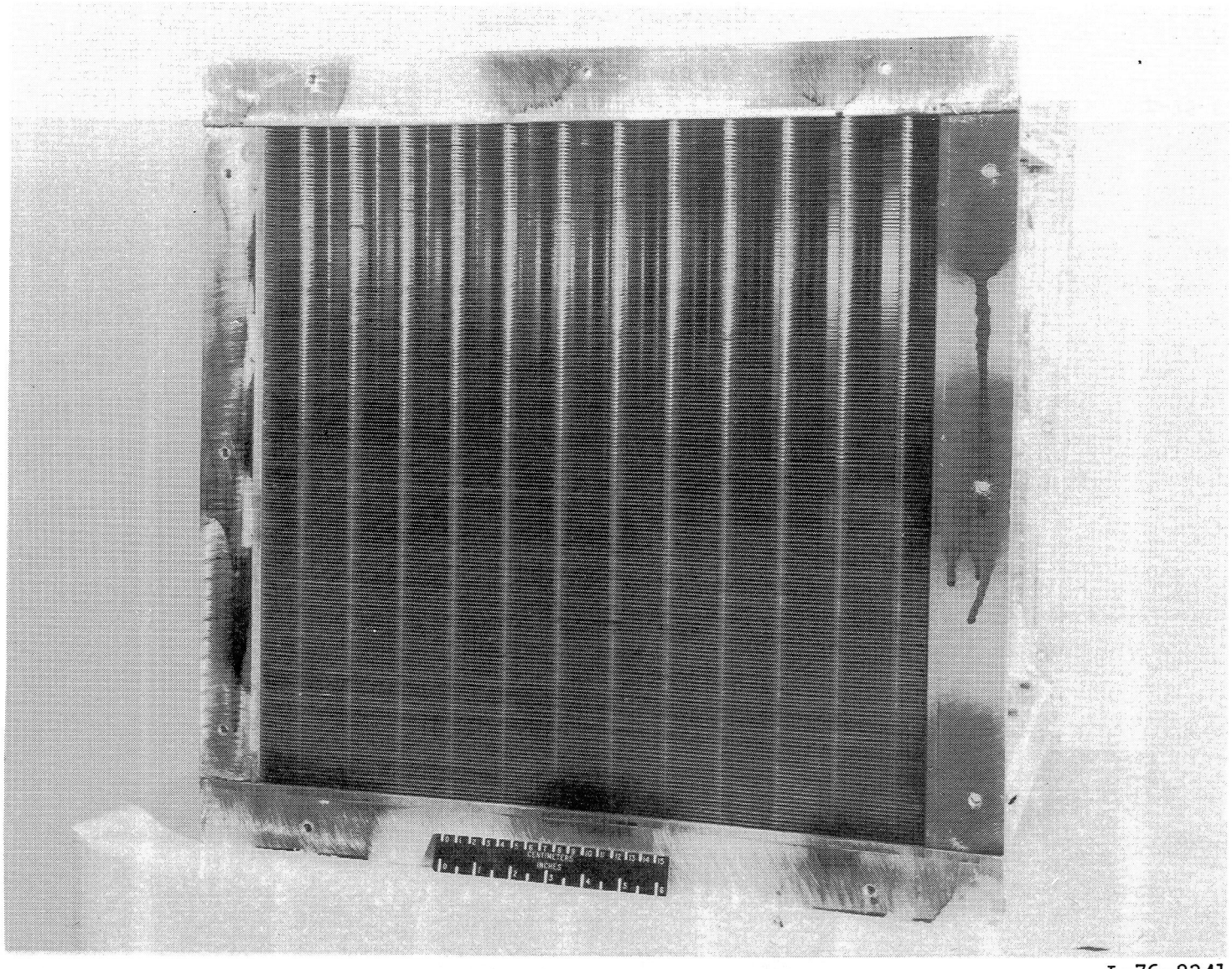

L-76-8241

(b) Photograph of complete tube bundle.

Figure 5.- Continued.

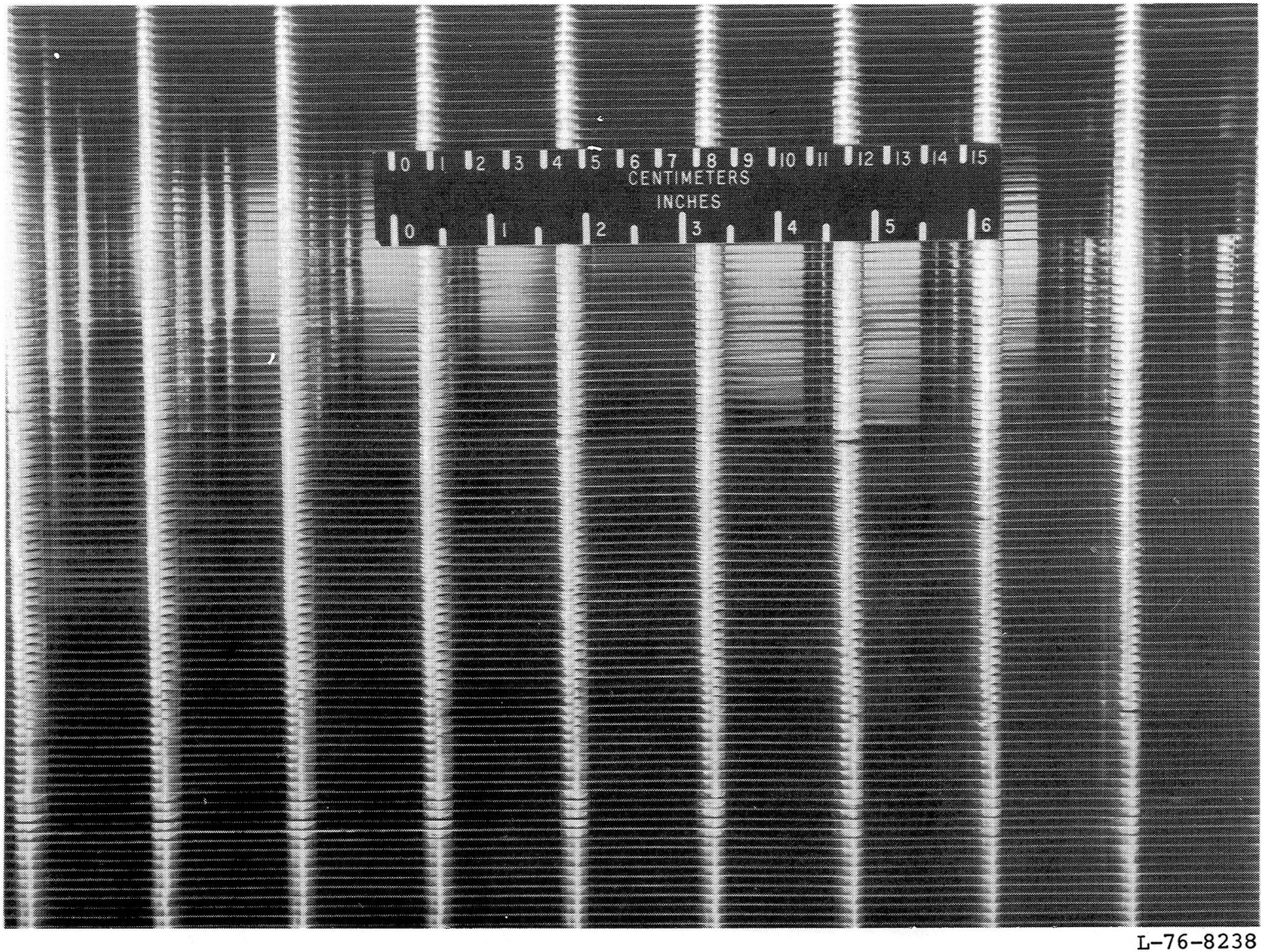

L-76-8238

(c) Detail photograph.

Figure 5.- Concluded.

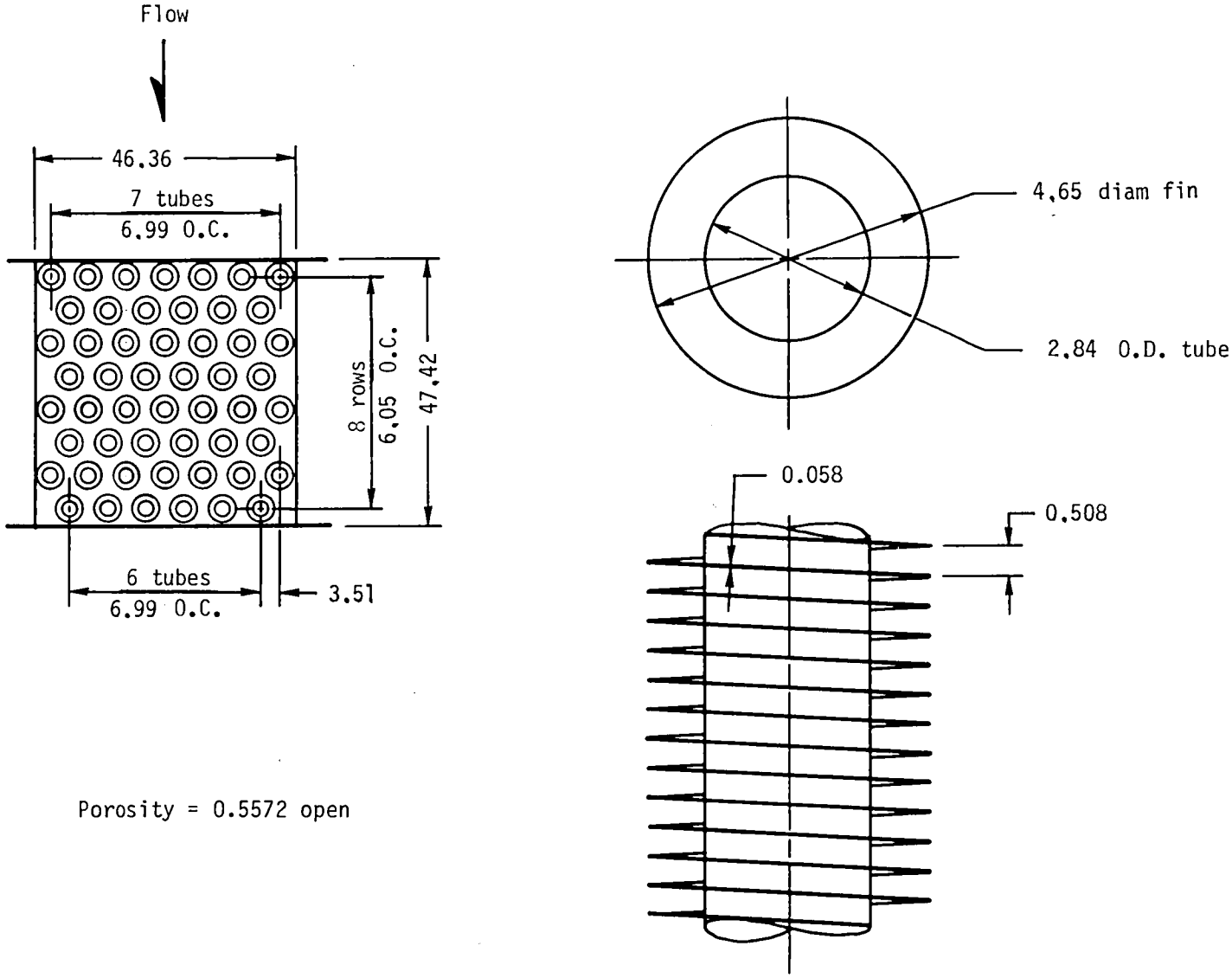

(a) Geometric details.

Figure 6.- Spiral-fin cooling-coil configuration. (All dimensions are in centimeters.)

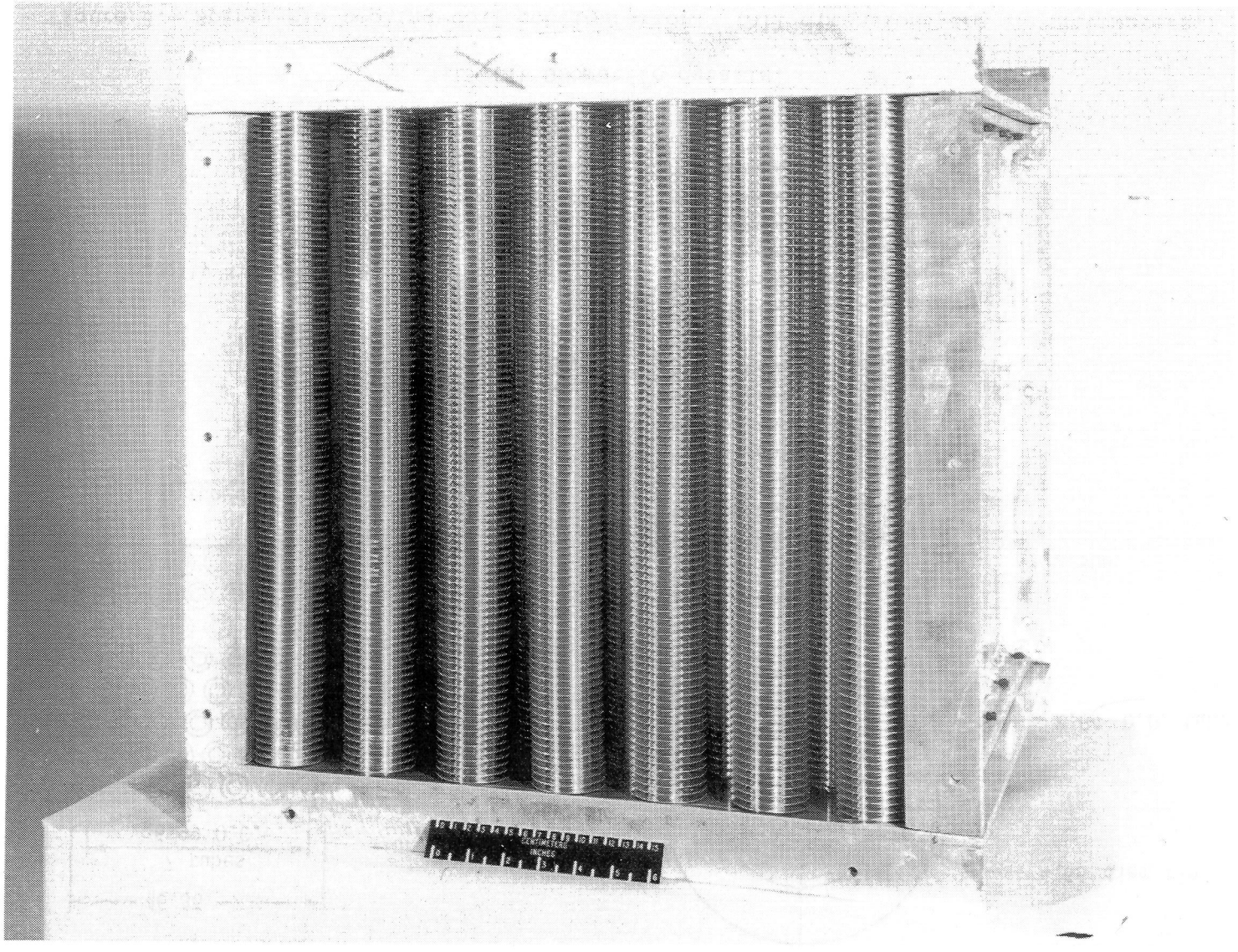

L-76-8246

(b) Photograph of complete tube bundle.

Figure 6.- Continued.

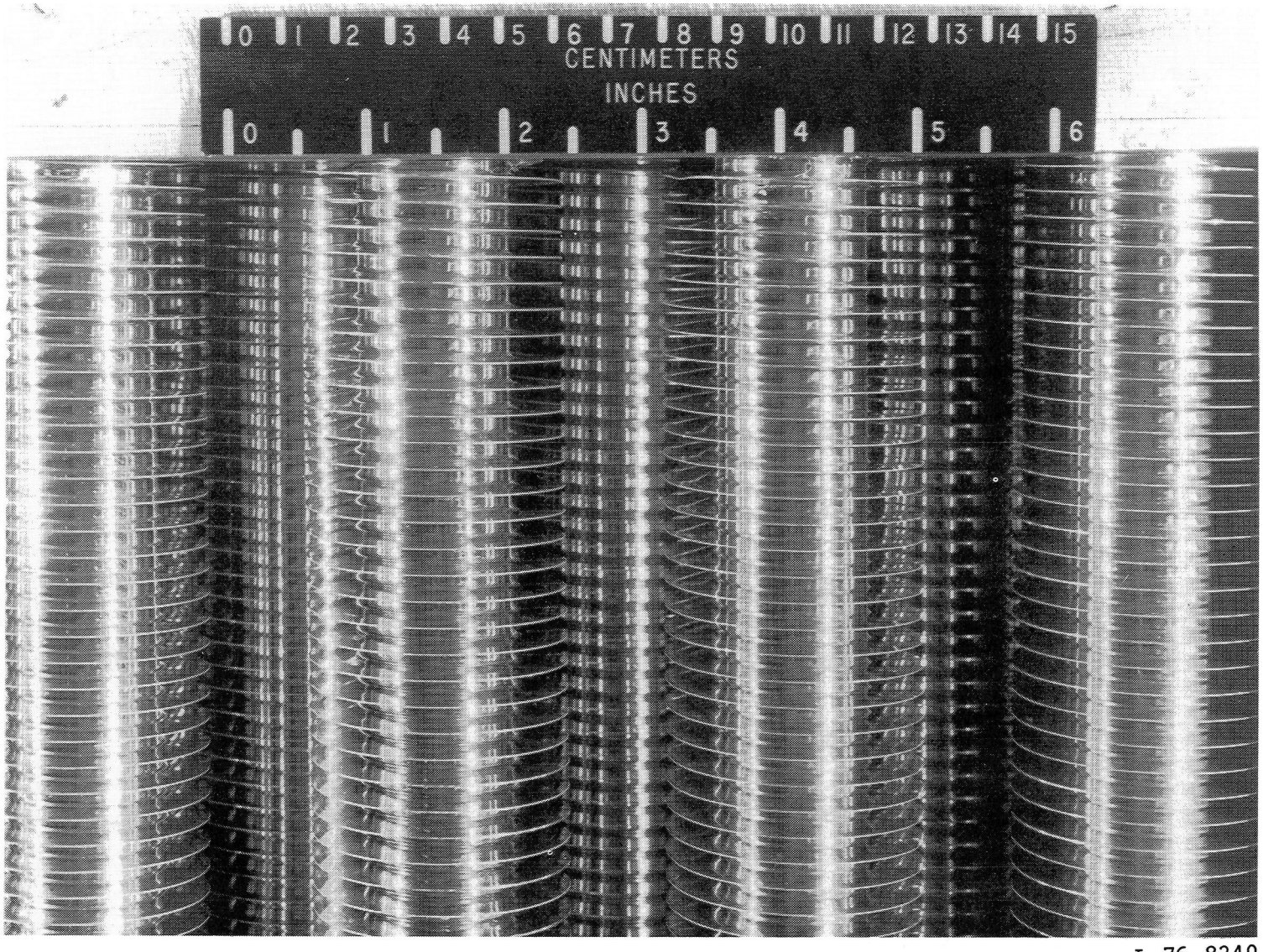

L-76-8240

(c) Detail photograph.

Figure 6.- Concluded.

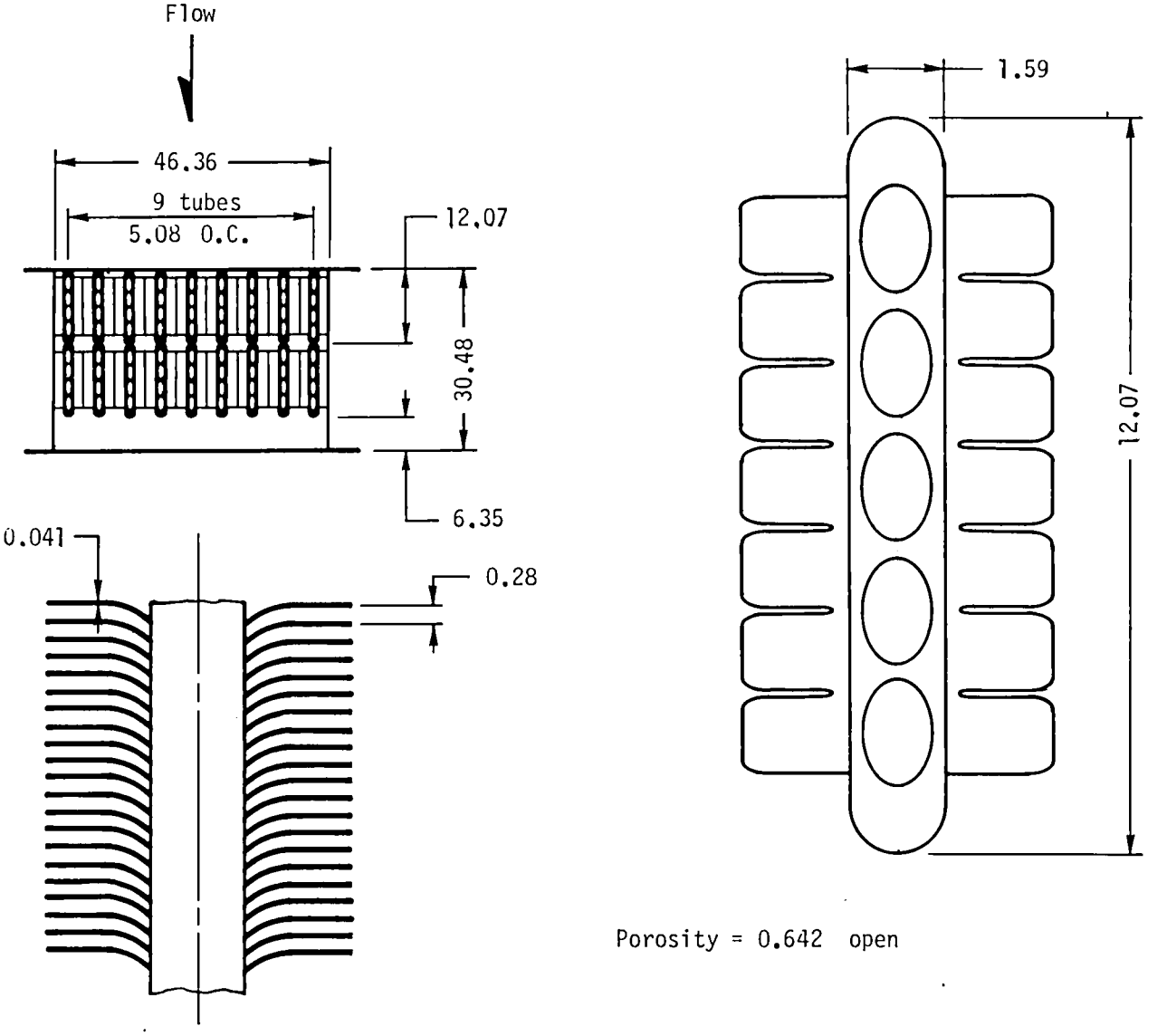

(a) Geometric details.

Figure 7.- Segmented-fin cooling-coil configuration. (All dimensions are in centimeters.)

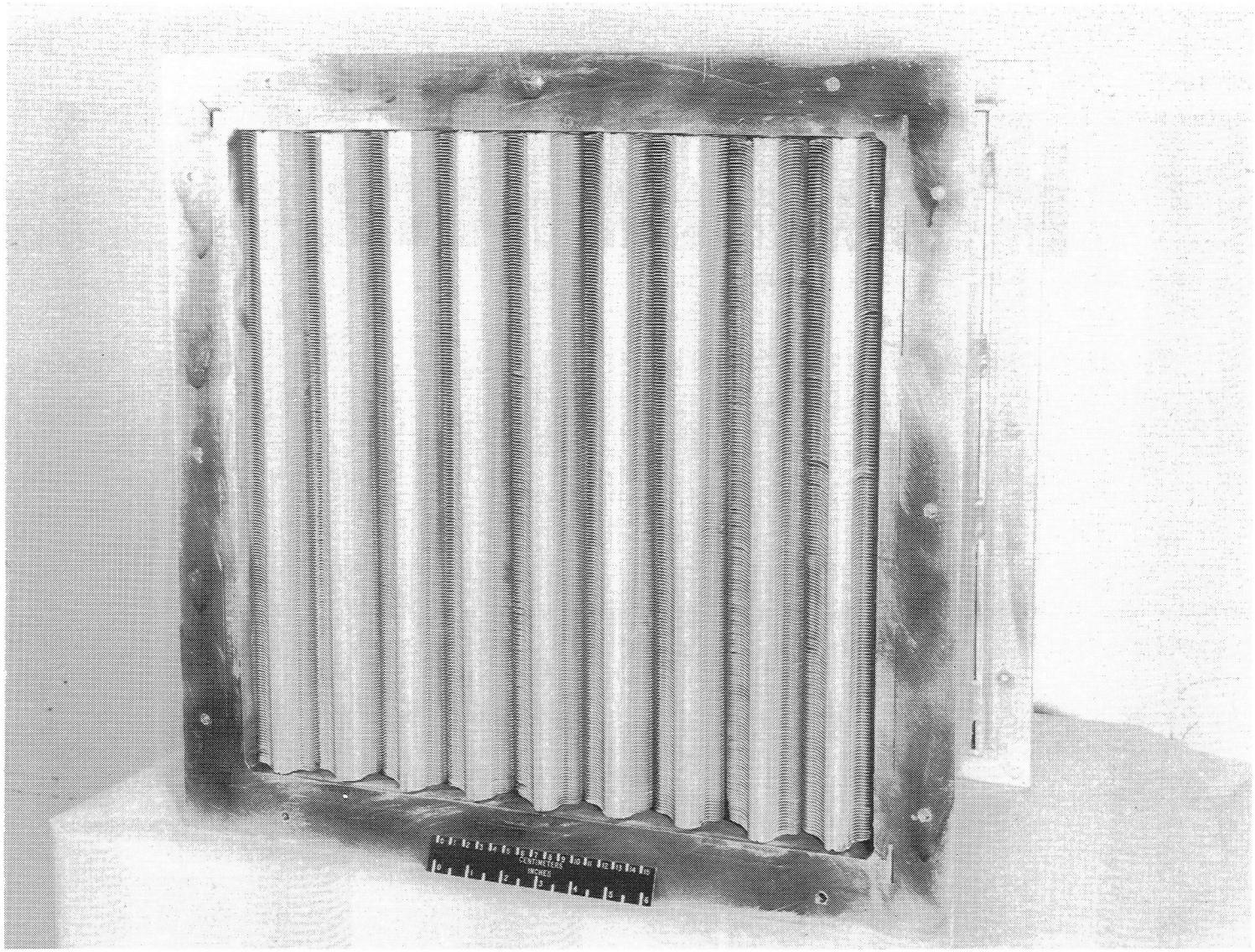

L-76-8253

(b) Photograph of complete tube bundle.

Figure 7.- Continued.

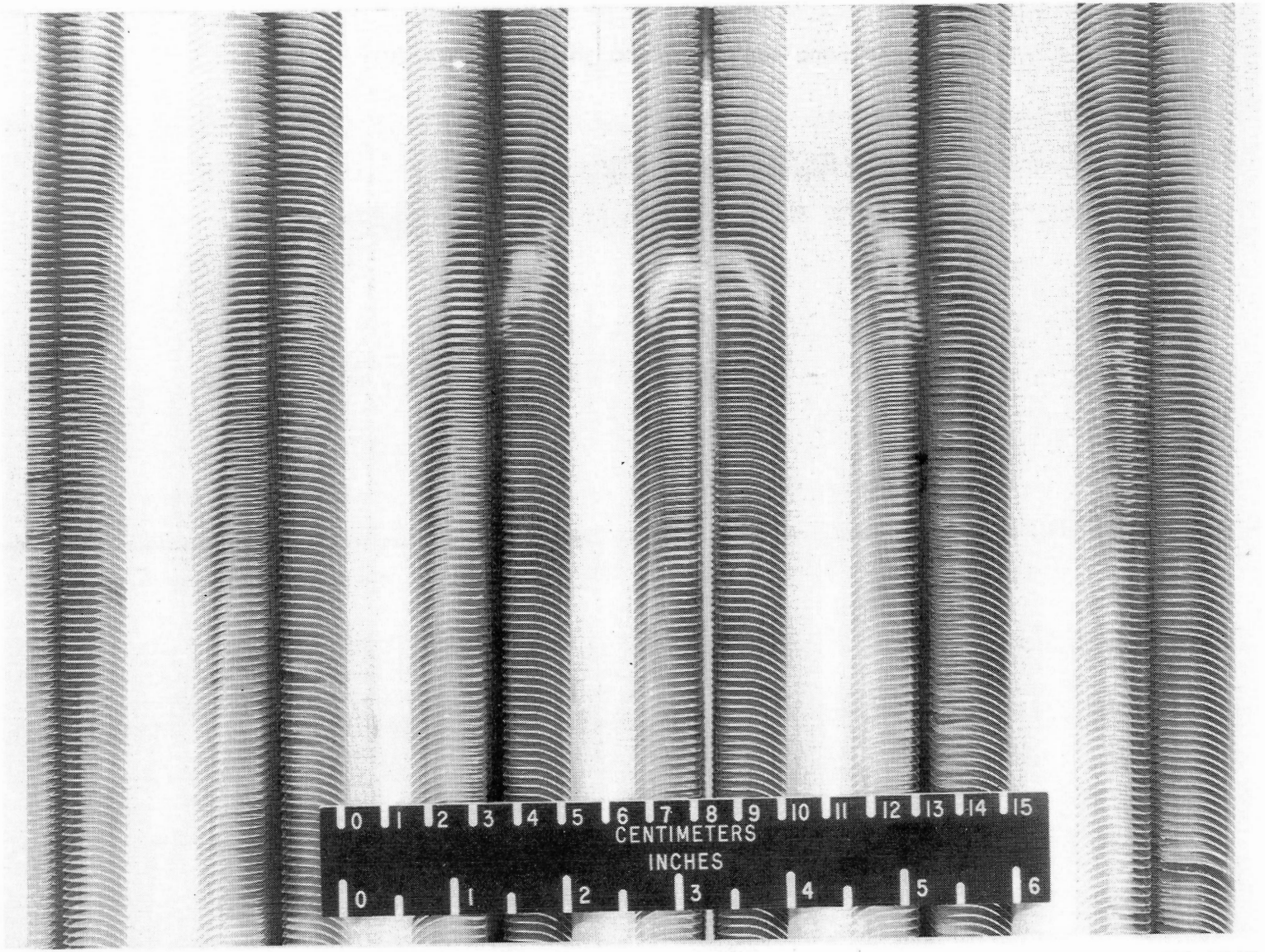

L-76-8247

(c) Detail photograph.

Figure 7.- Concluded.

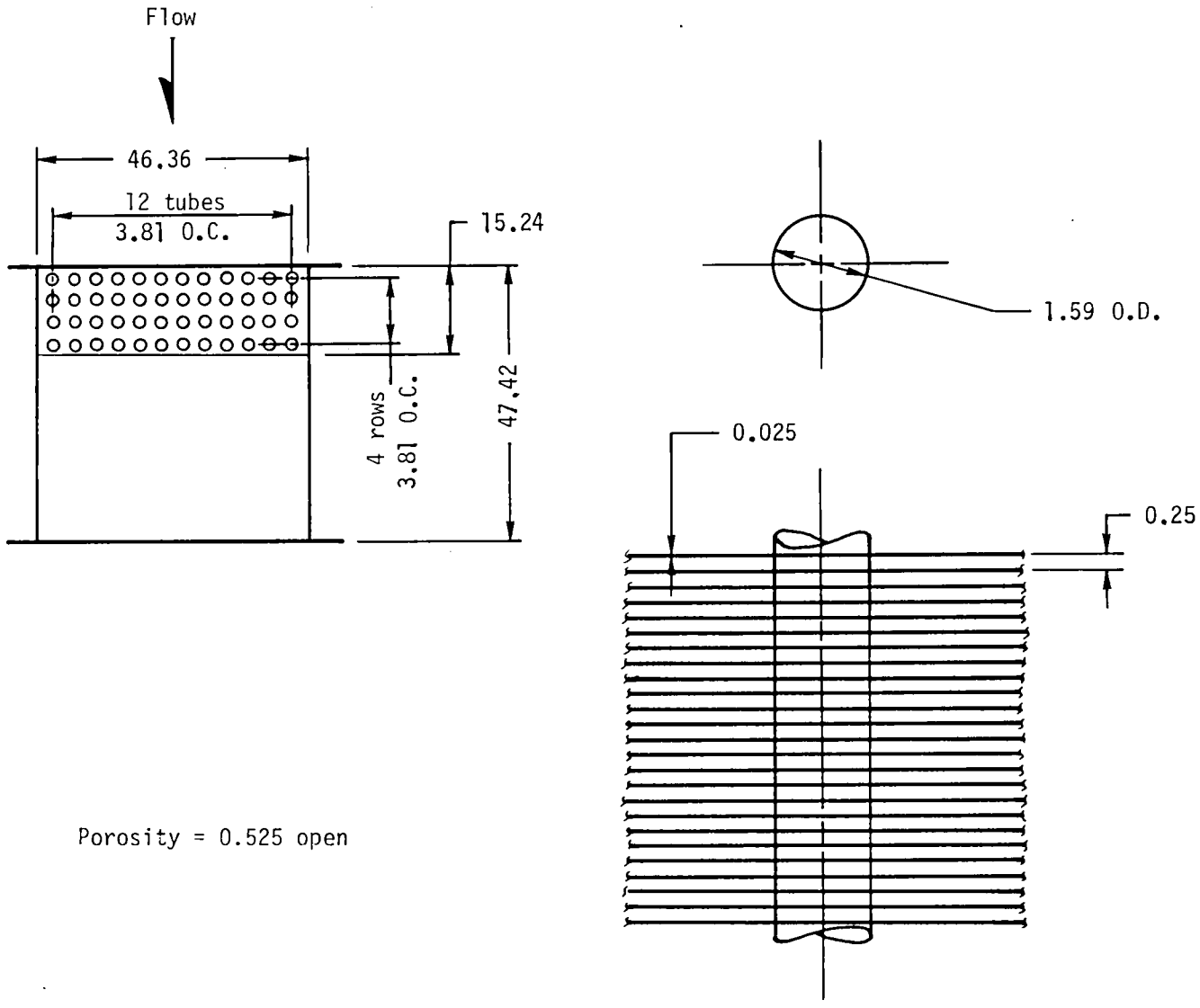

Figure 8.- Baseline cooling-coil configuration. (All dimensions are in centimeters.)

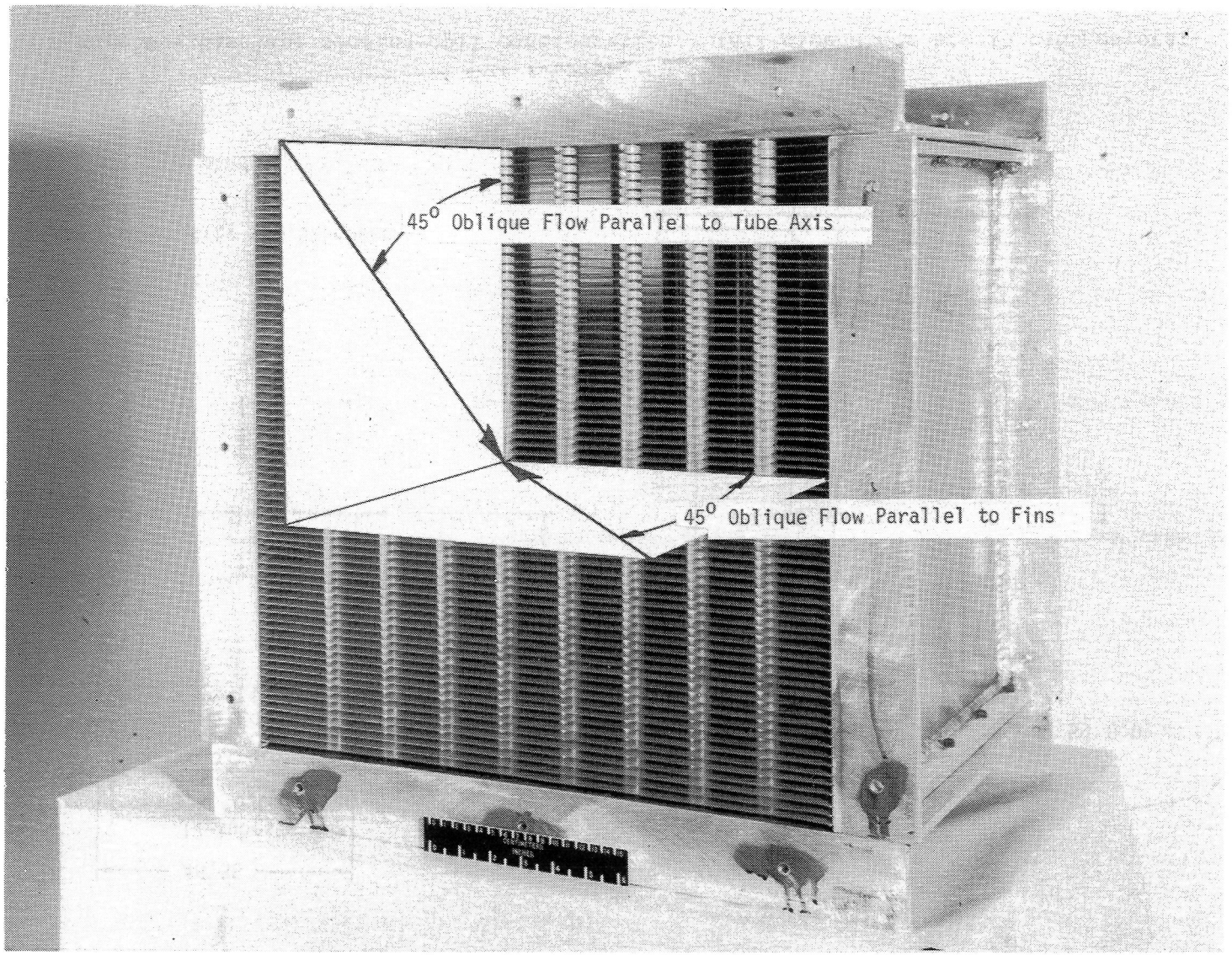

L-76-8248.1

Figure 9.- Flow directions for oblique flow tests.

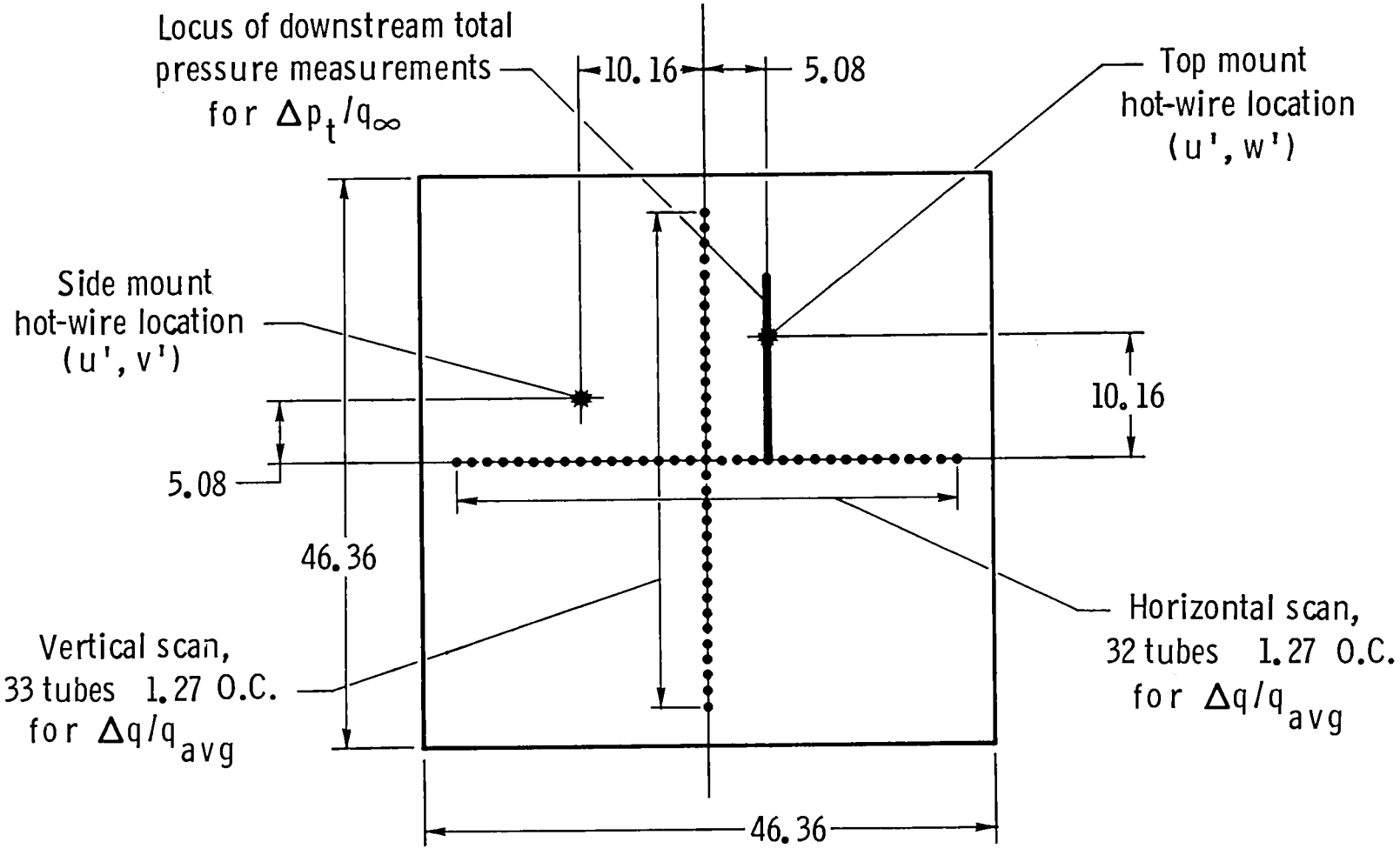

Figure 10.- Instrumentation location and arrangement facing upstream.
(All dimensions are in centimeters.)

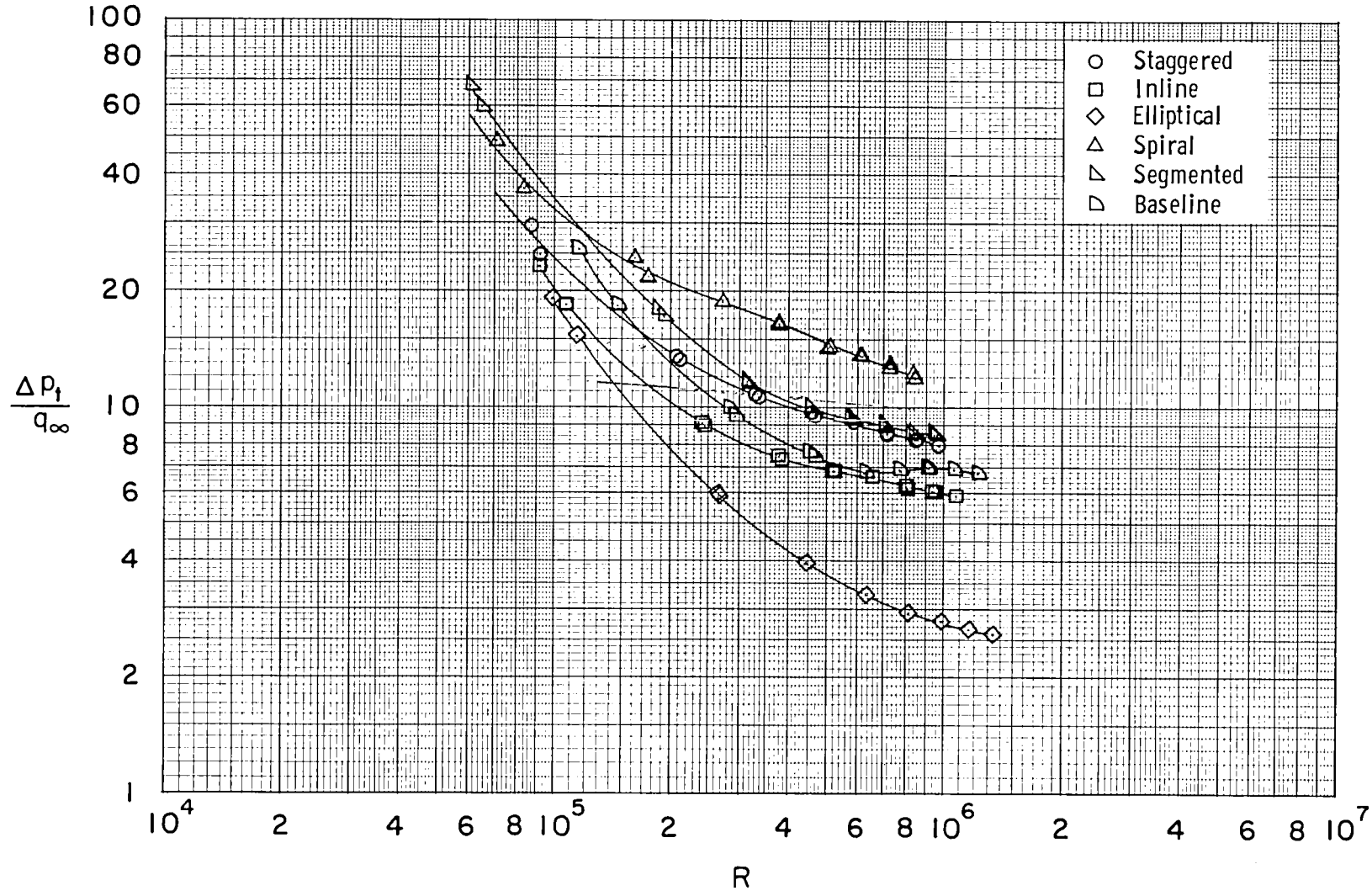

Figure 11.- Pressure-drop characteristics of cooling-coil configurations in normal flow.

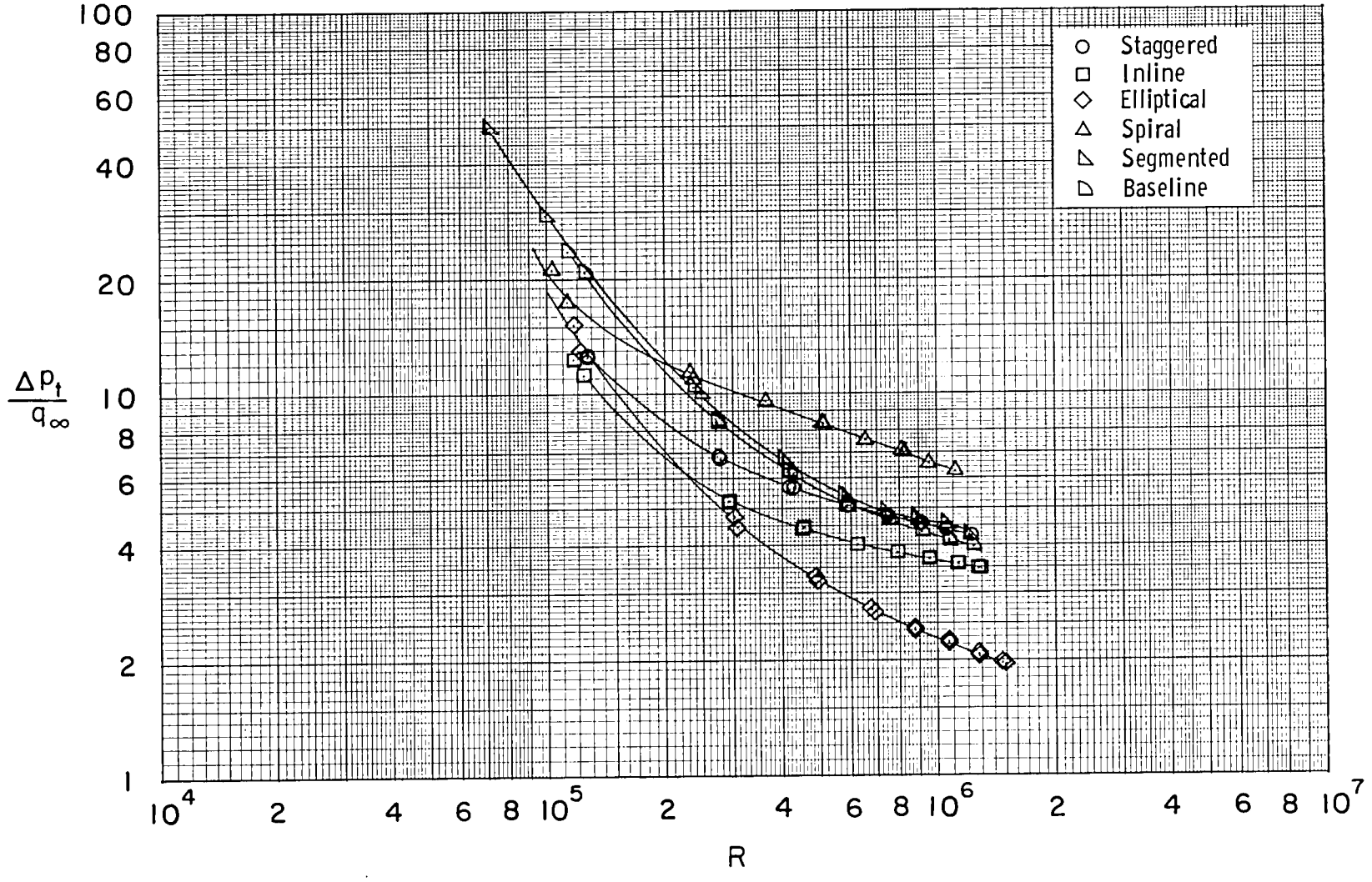

Figure 12.- Pressure-drop characteristics of cooling-coil configurations in 45° oblique flow parallel to fins.

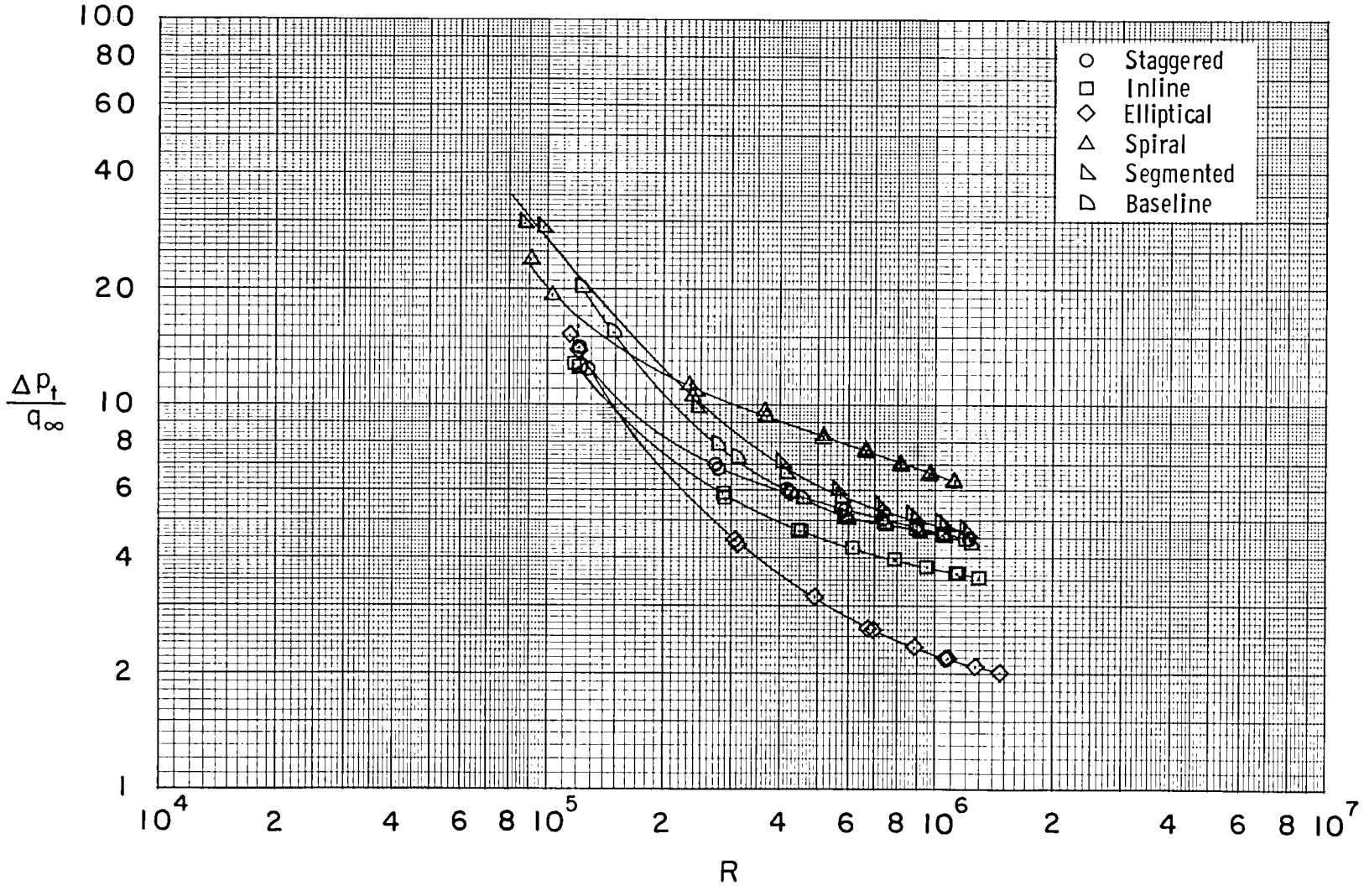

Figure 13.- Pressure-drop characteristics of cooling-coil configurations in 45^o oblique flow parallel to tube axis.

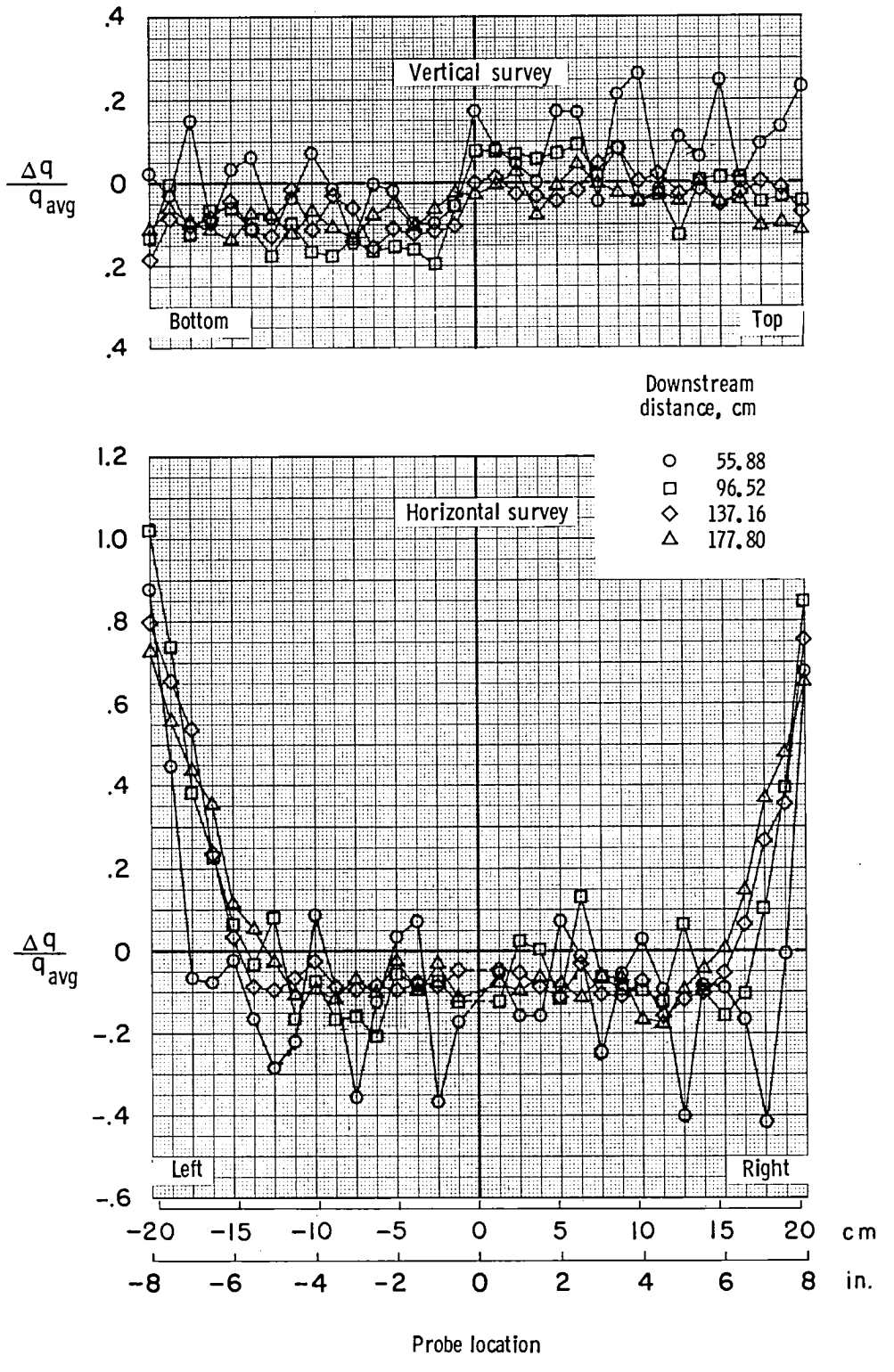

(a) Normal flow; $R \approx 0.97 \times 10^6$.

Figure 14.- Flow uniformity at four downstream survey stations for staggered cooling-coil configuration.

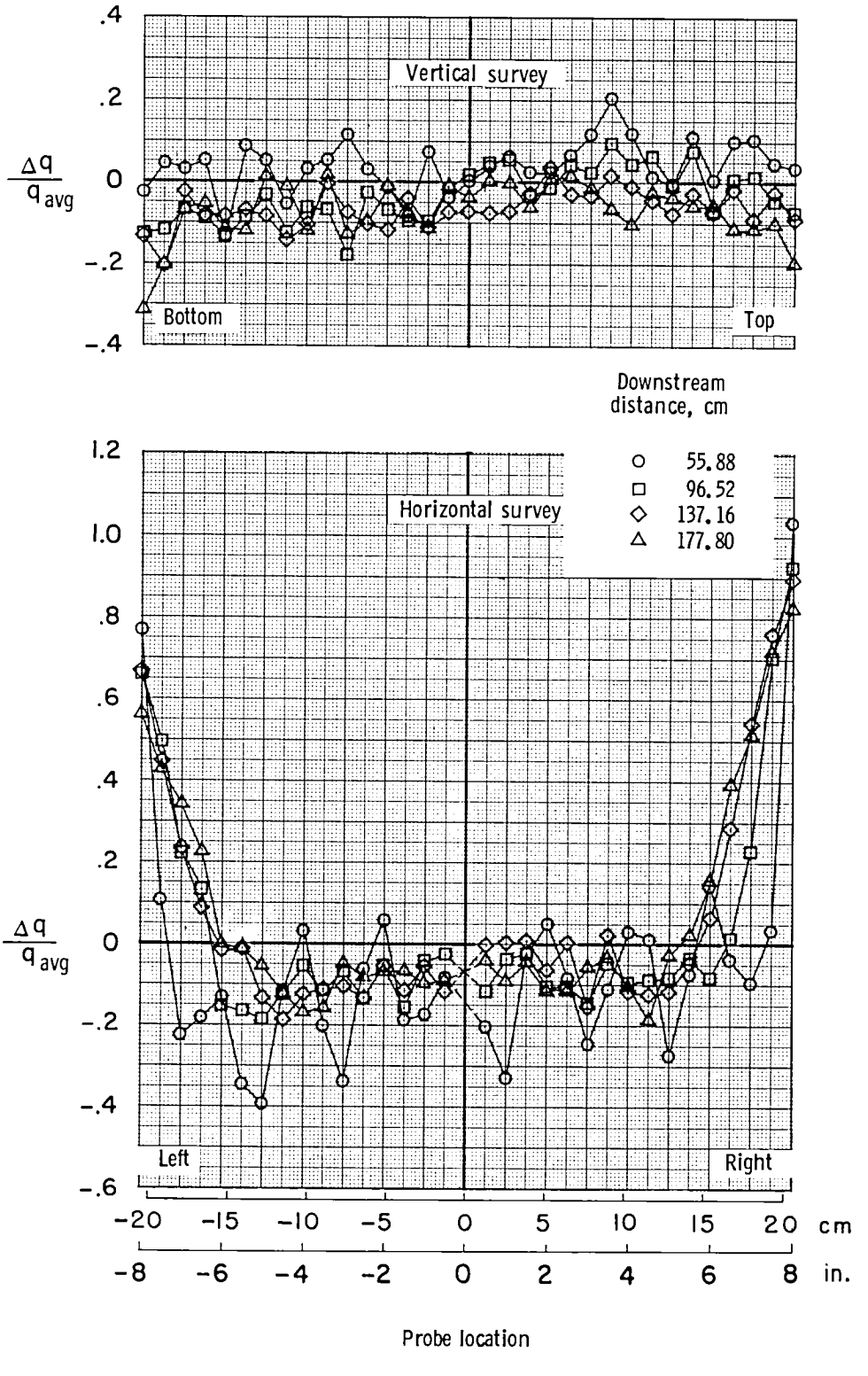

(b) 45^{o} oblique flow parallel to fins; $R \approx 1.23 \times 10^{6}$.

Figure 14.- Continued.

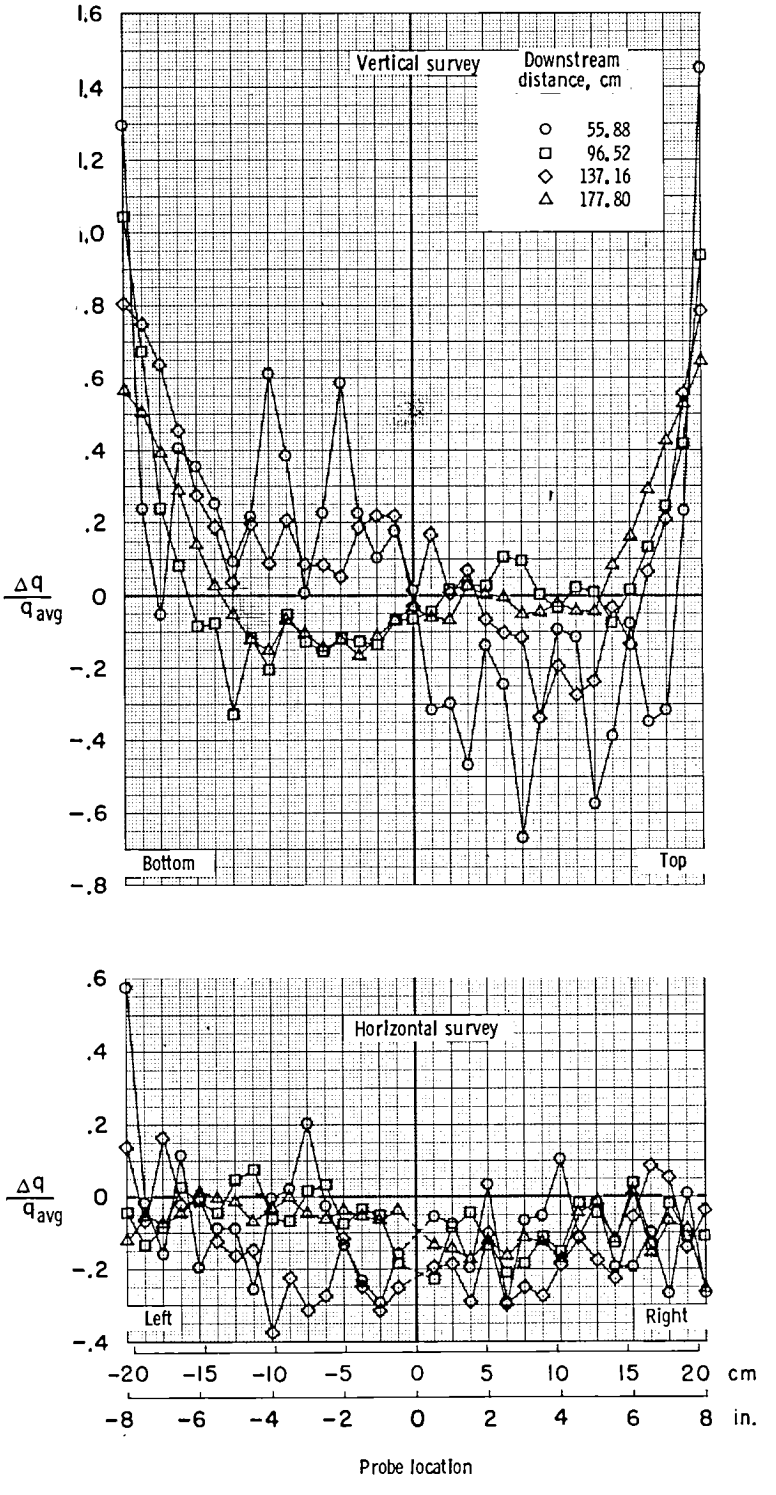

(c) 45° oblique flow parallel to tube axis; $R \approx 1.22 \times 10^6$.

Figure 14.- Concluded.

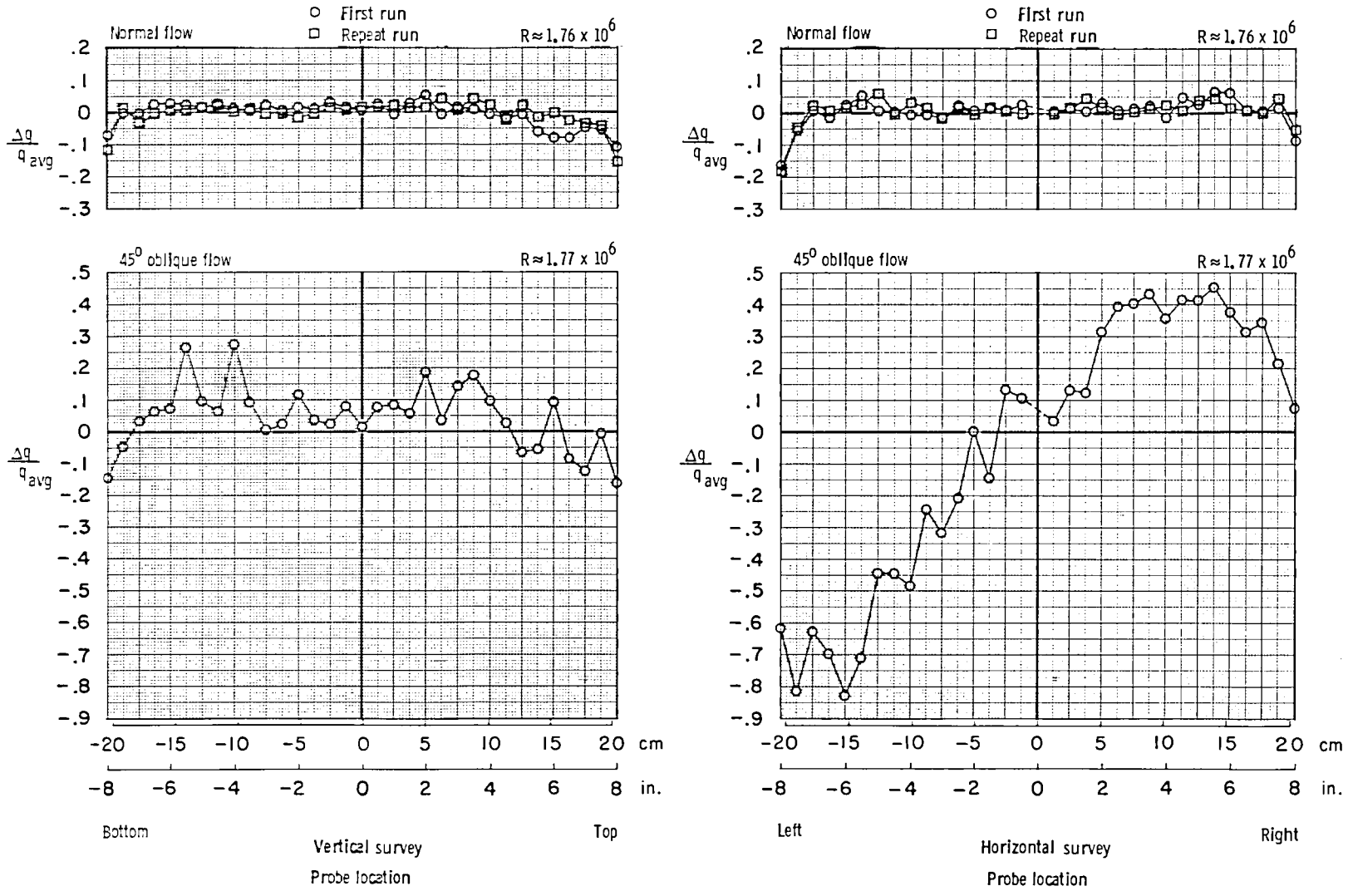

Figure 15.- Flow uniformity at 1.78-m station for clear duct.

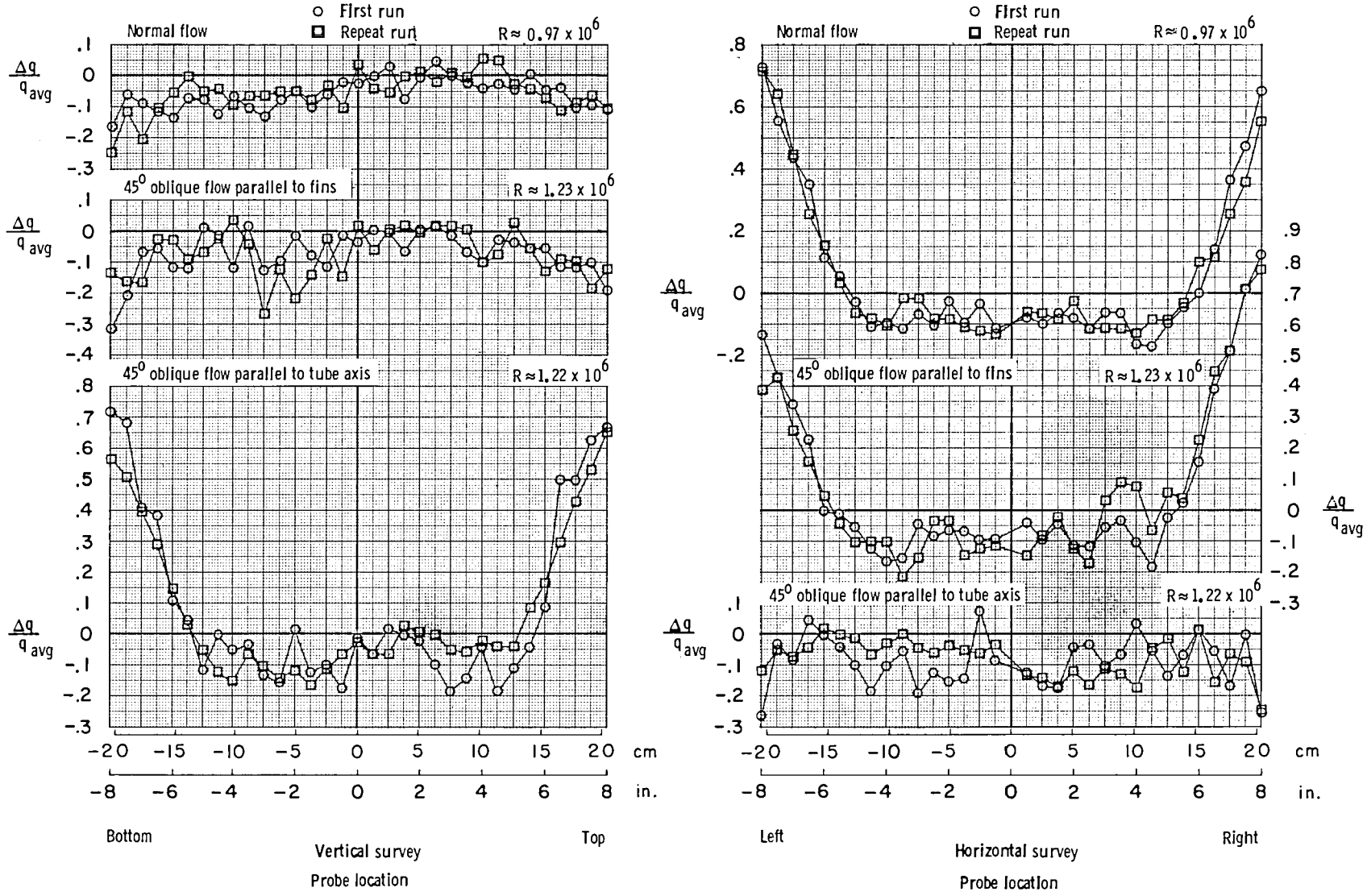

Figure 16.- Flow uniformity at 1.78-m station for staggered cooling-coil configuration.

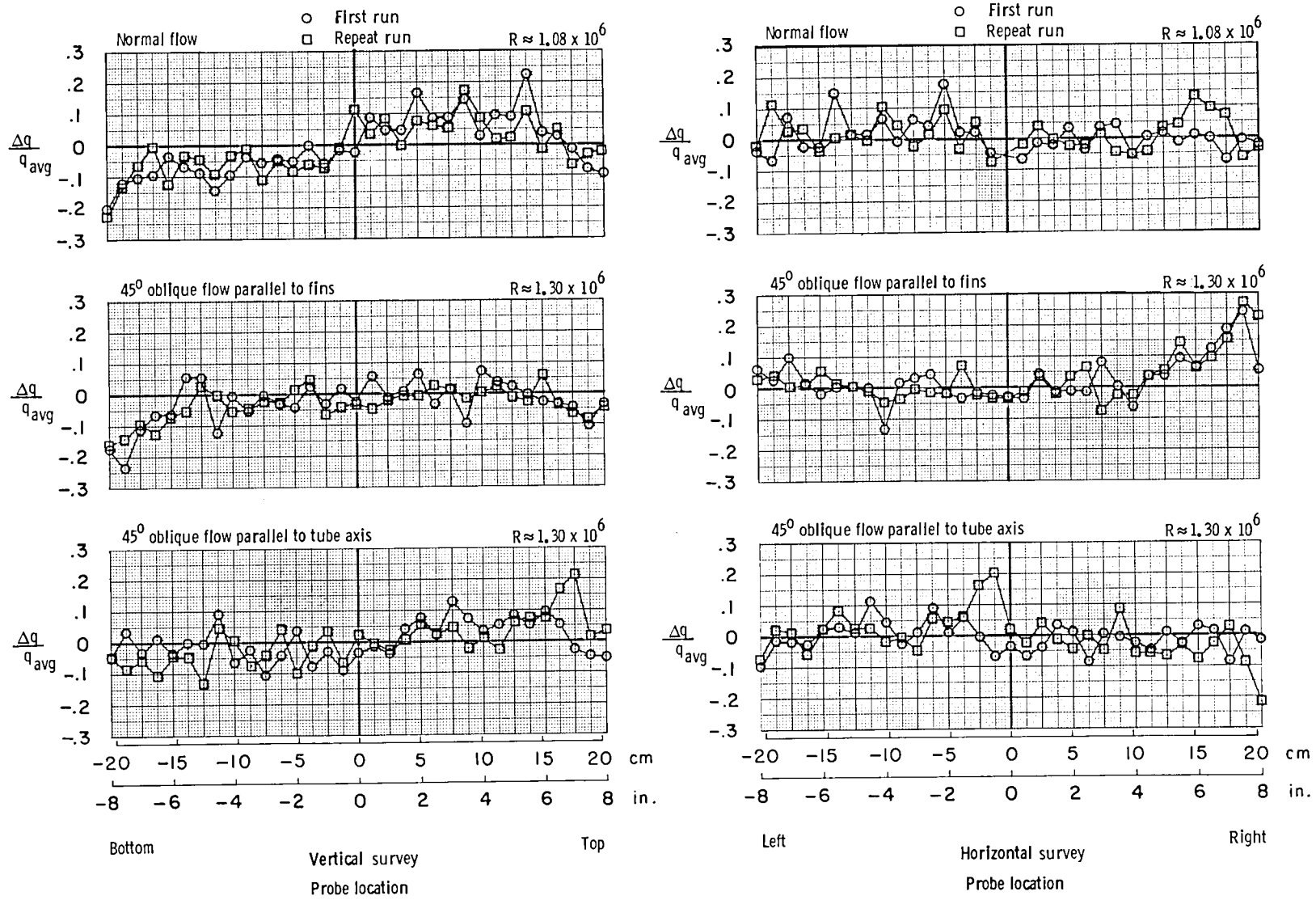

Figure 17.- Flow uniformity at 1.78-m station for inline cooling-coil configuration.

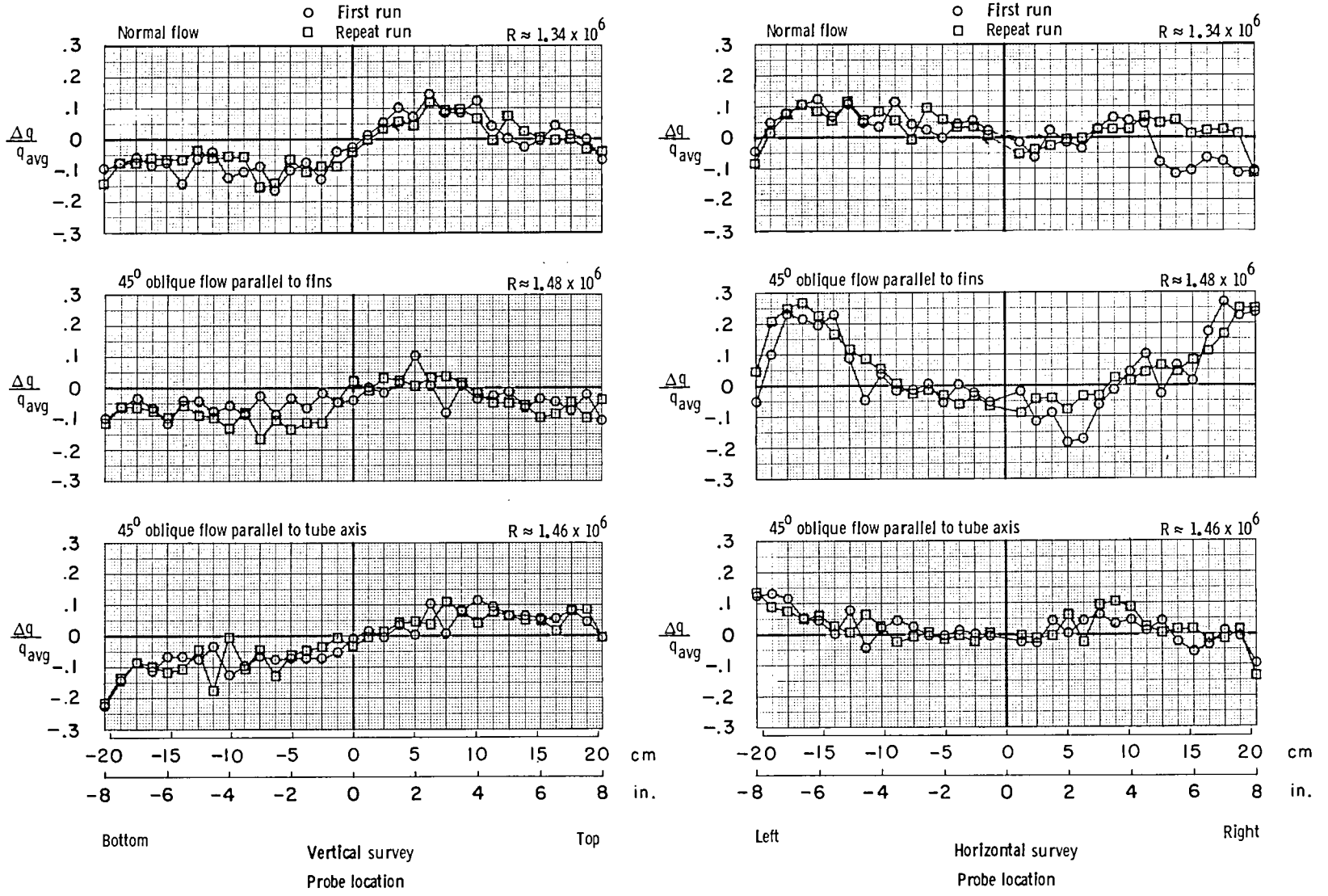

Figure 18.- Flow uniformity at 1.78-m station for elliptical cooling-coil configuration.

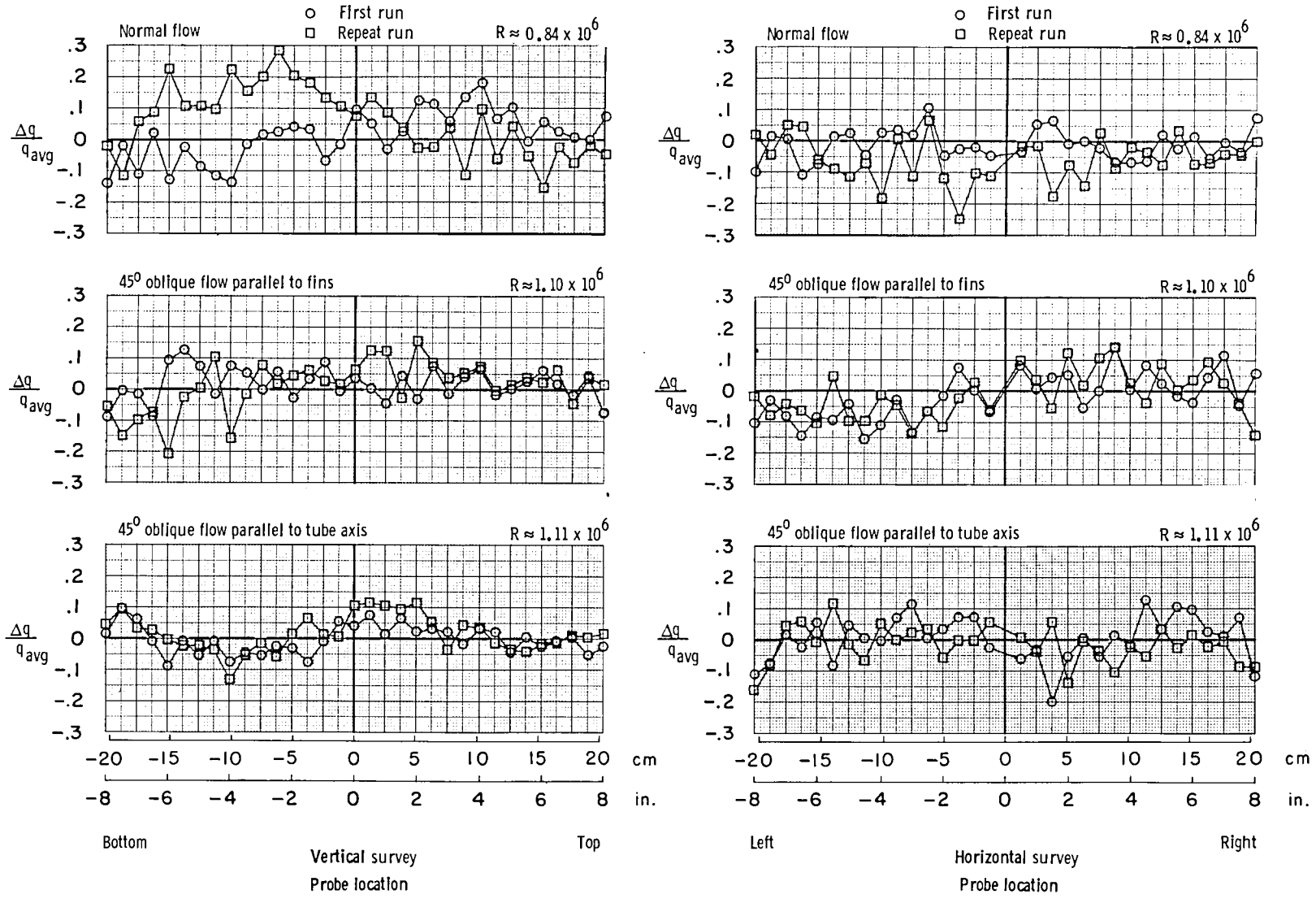

Figure 19.- Flow uniformity at 1.78-m station for spiral cooling-coil configuration.

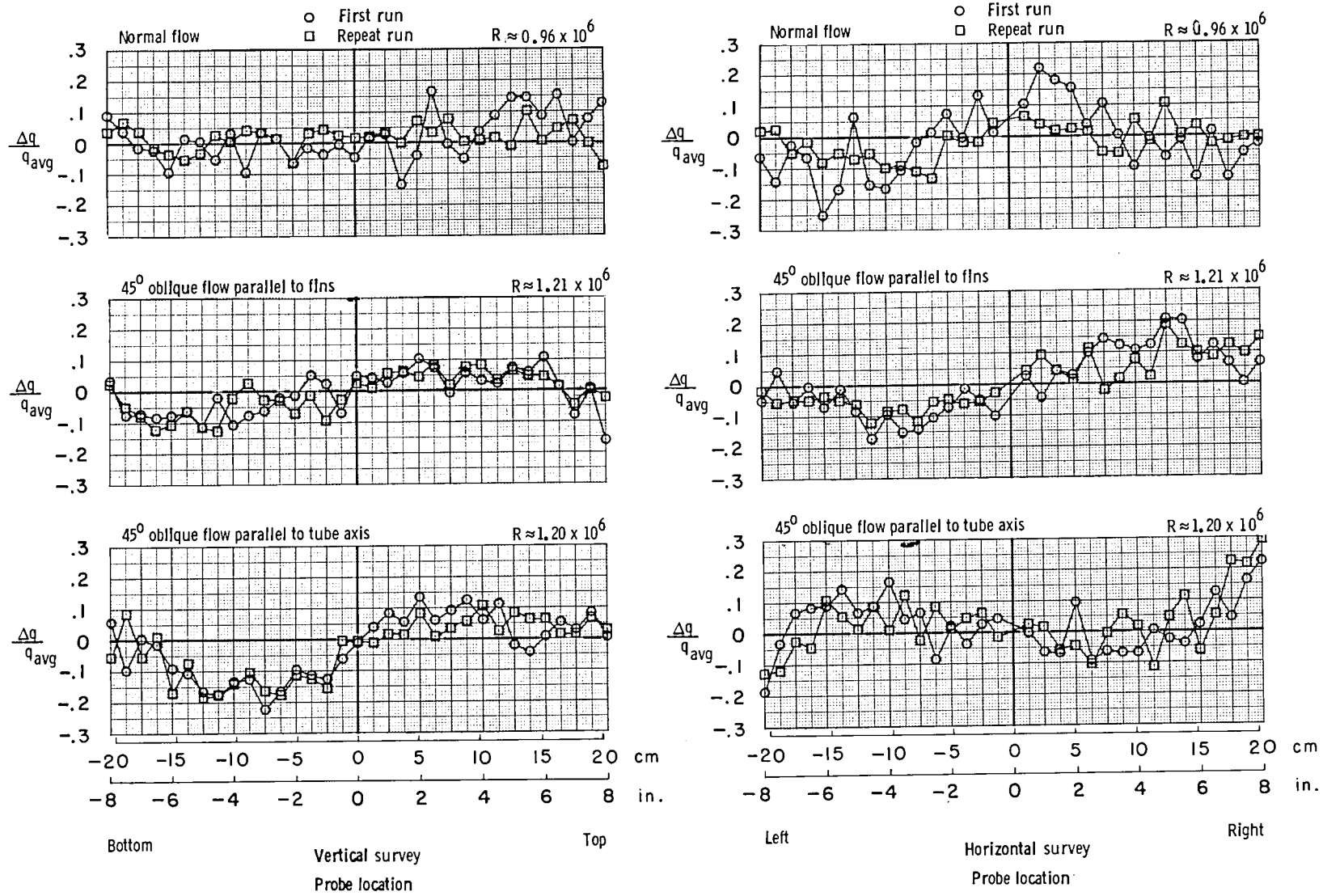

Figure 20.- Flow uniformity at 1.78-m station for segmented cooling-coil configuration.

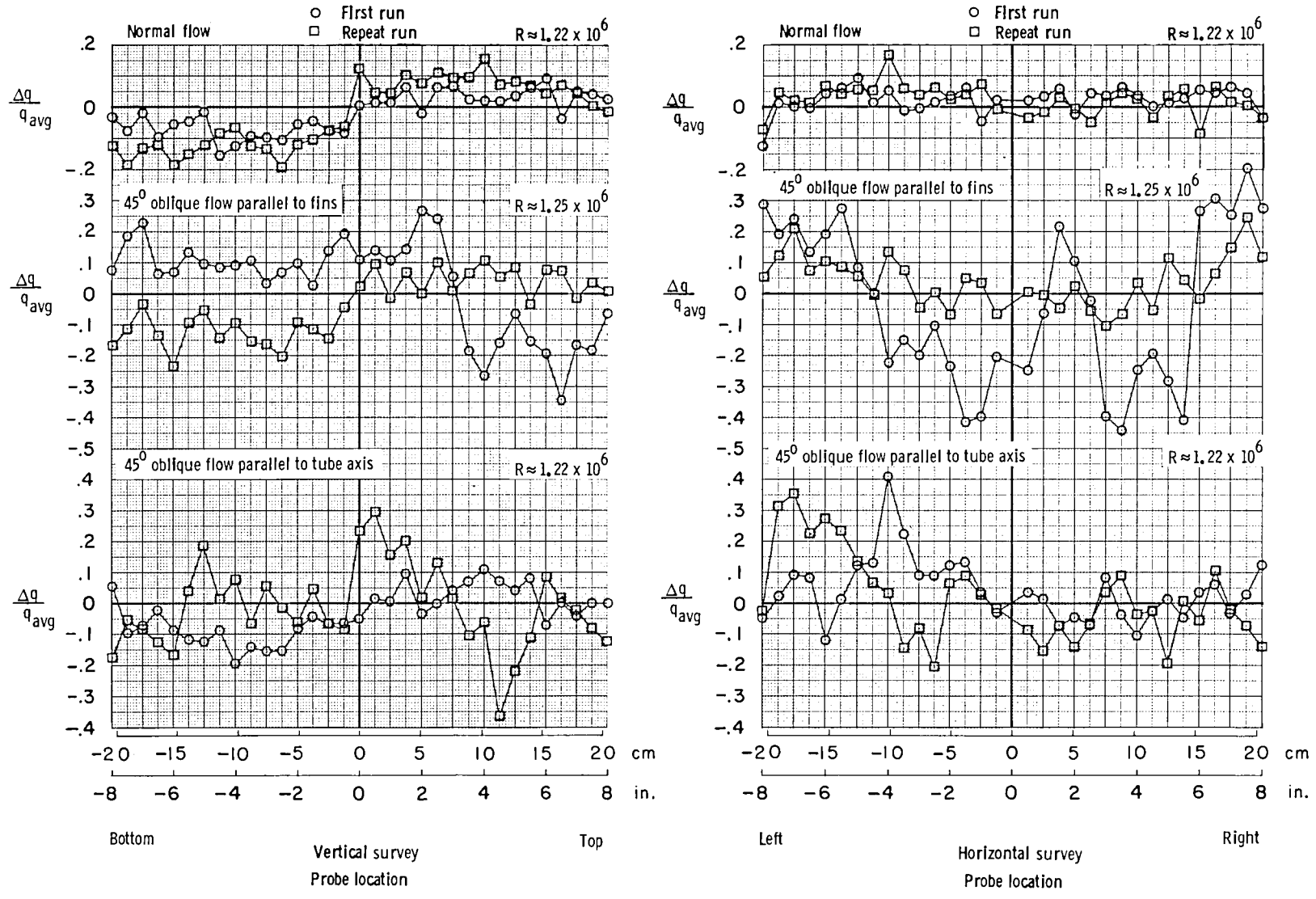

Figure 21.- Flow uniformity at 1.78-m station for baseline cooling-coil configuration.

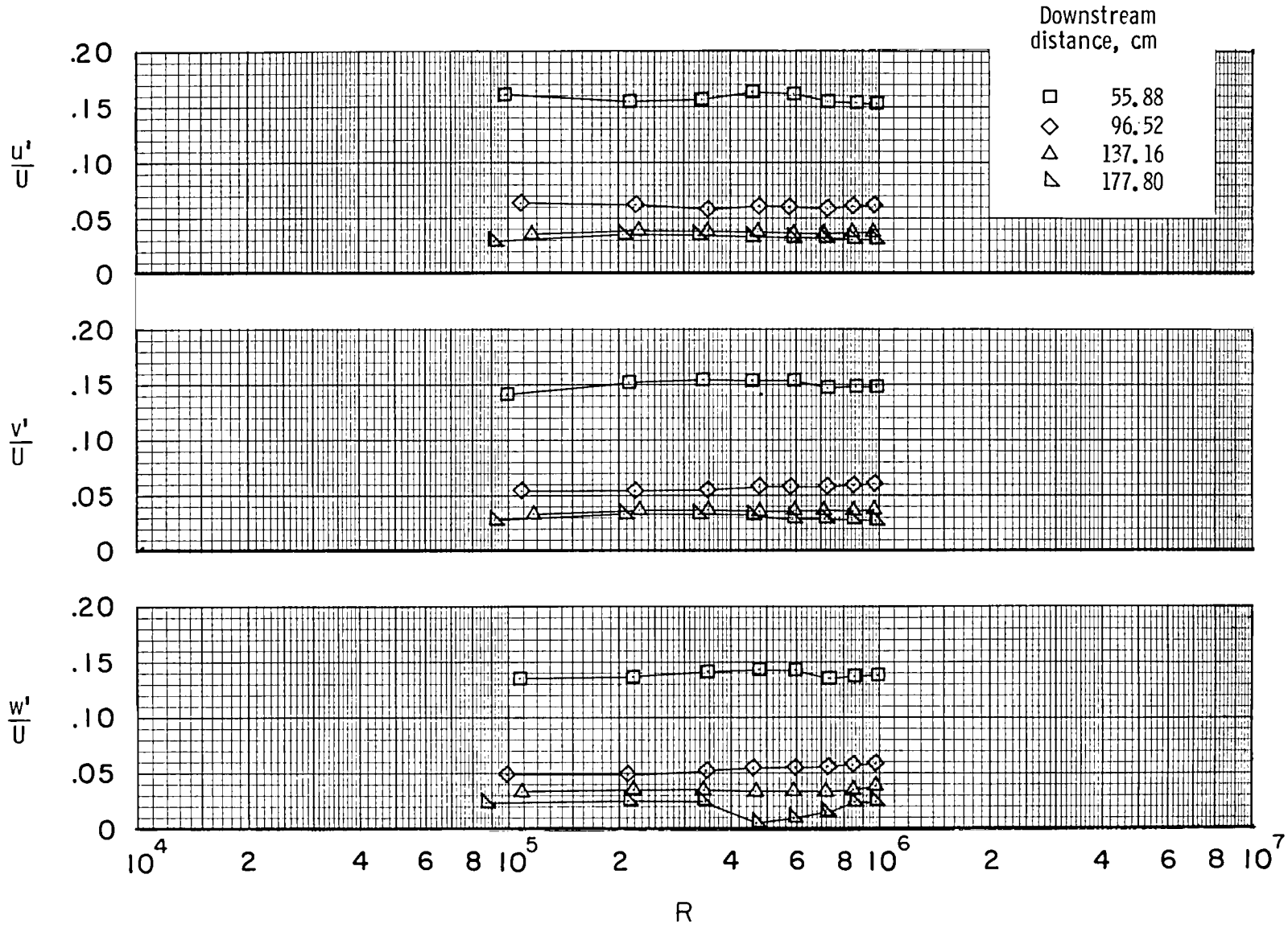

(a) Normal flow.

Figure 22.- Decay of turbulence levels behind staggered cooling-coil configuration.

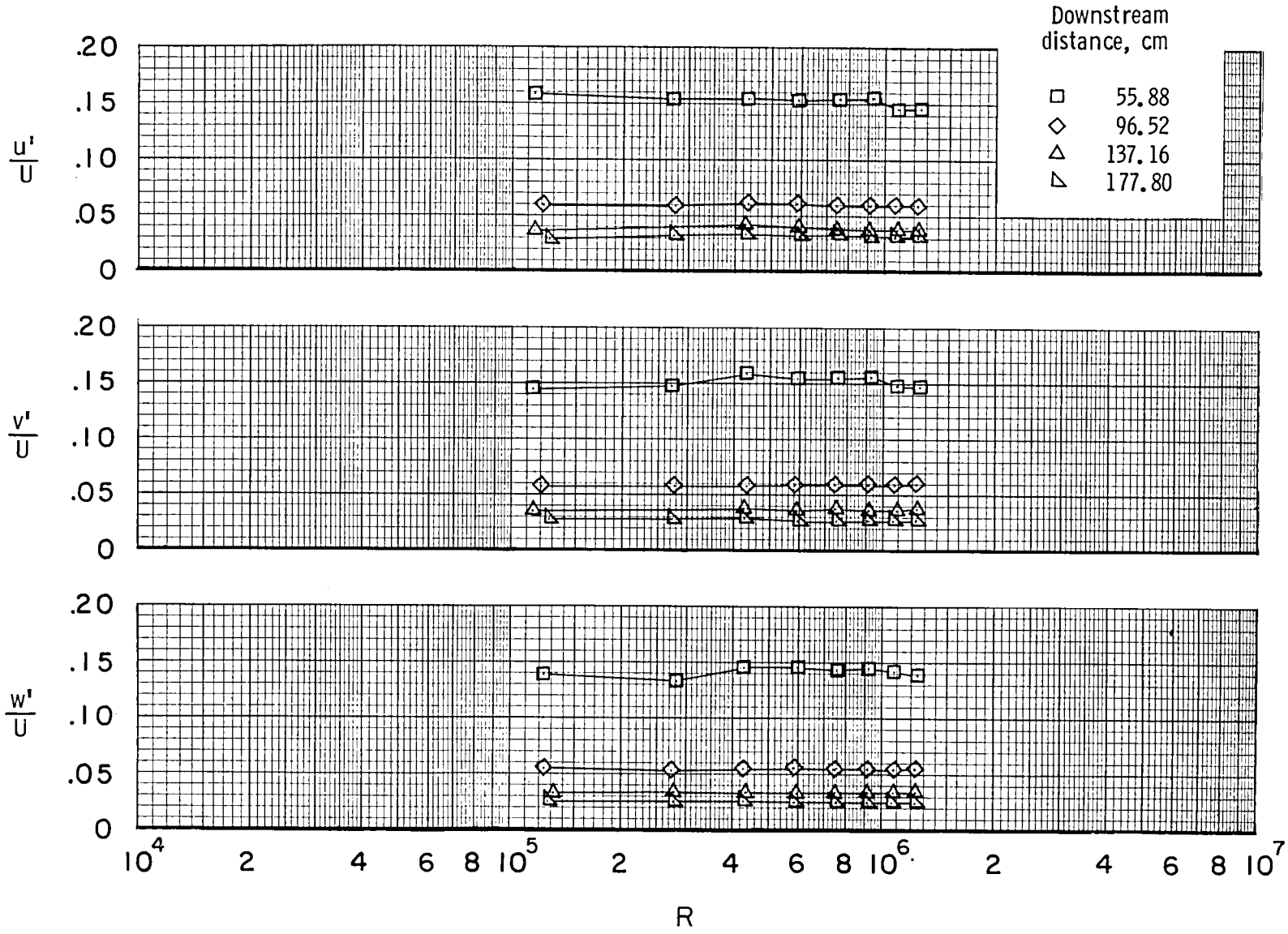

(b) 45° oblique flow parallel to fins.

Figure 22.- Continued.

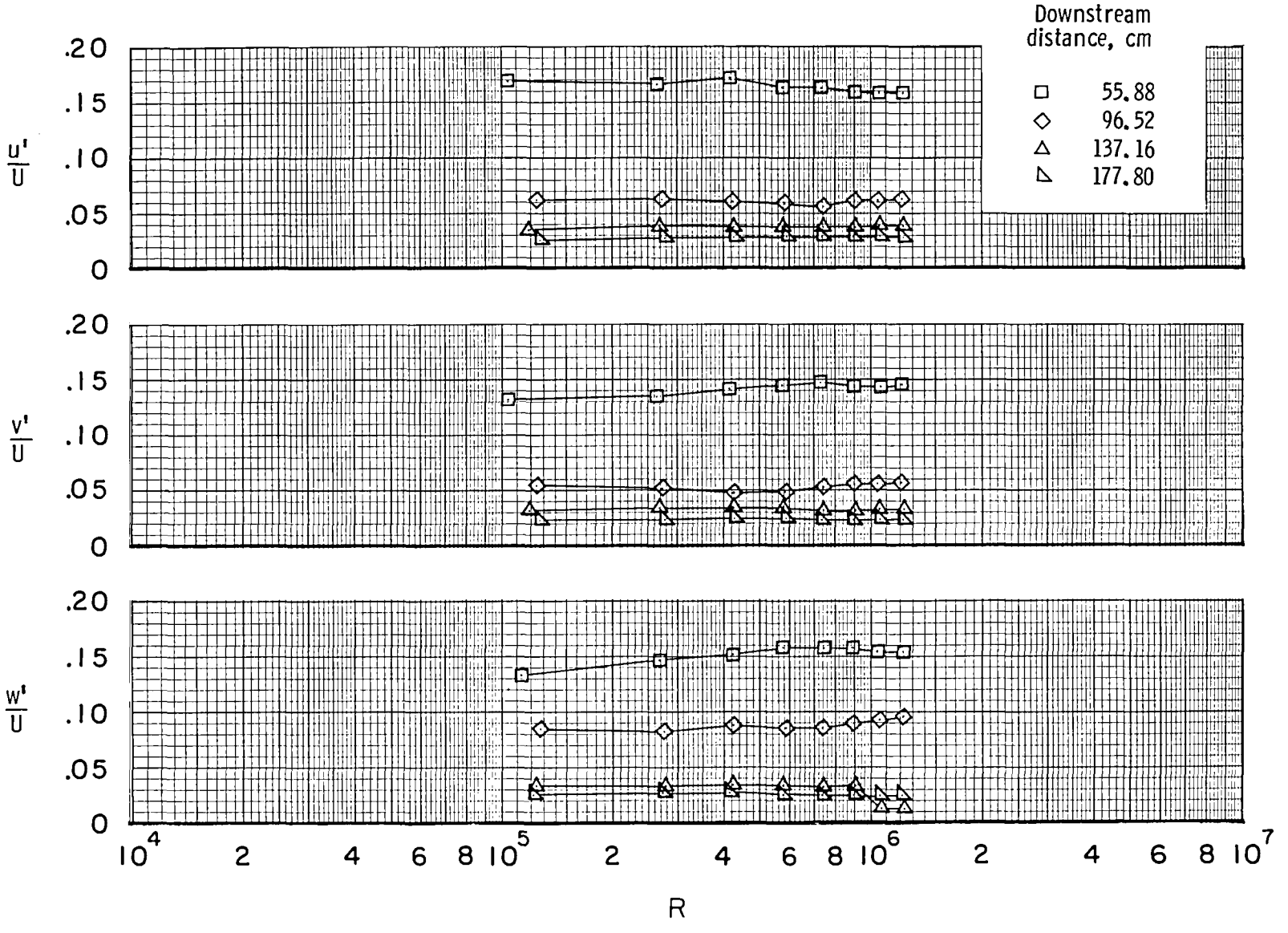

(c) 45° oblique flow parallel to tube axis.

Figure 22.- Concluded.

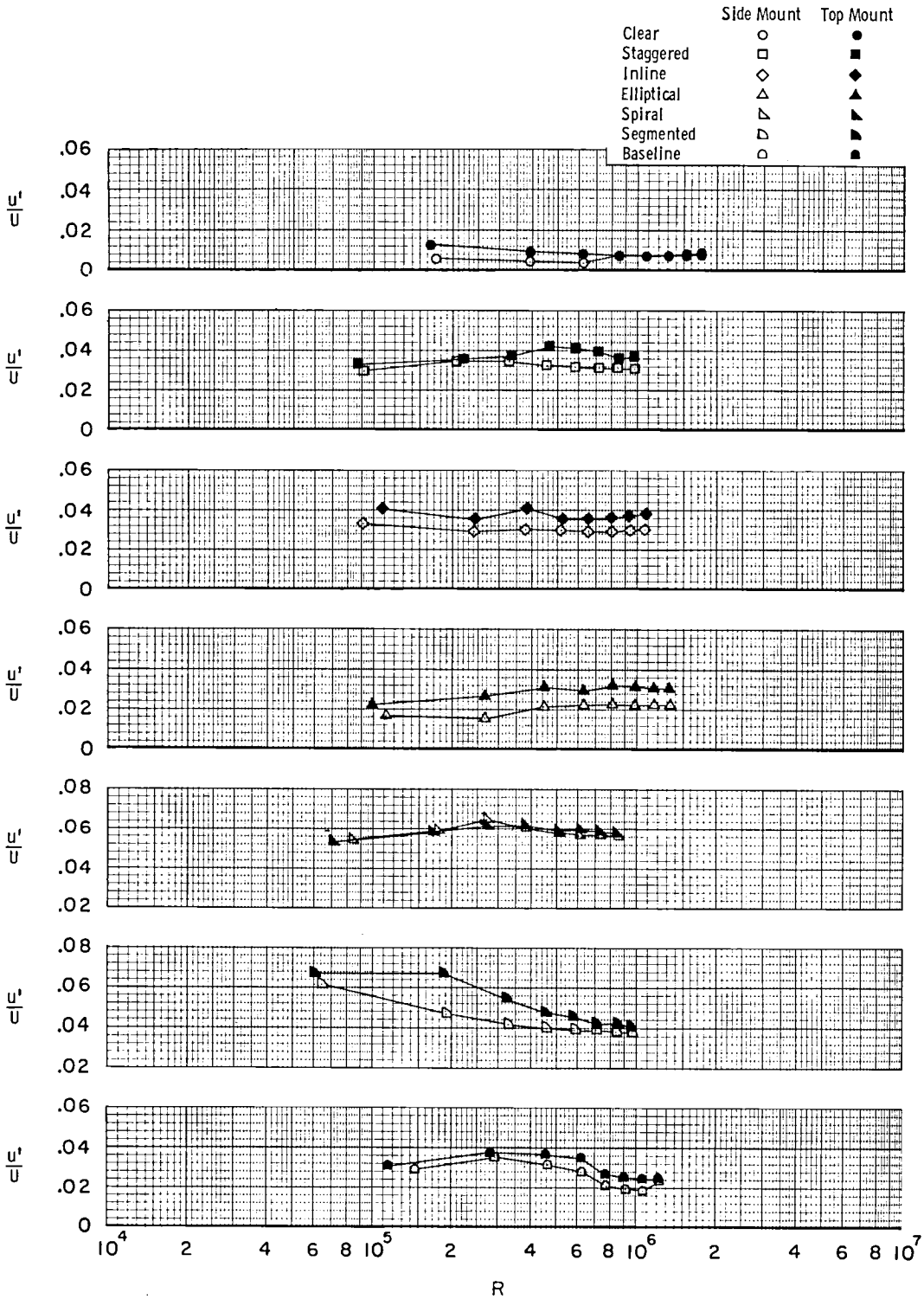

Figure 23.- Homogeneity of longitudinal turbulence with flow normal to cooling-coil configurations.

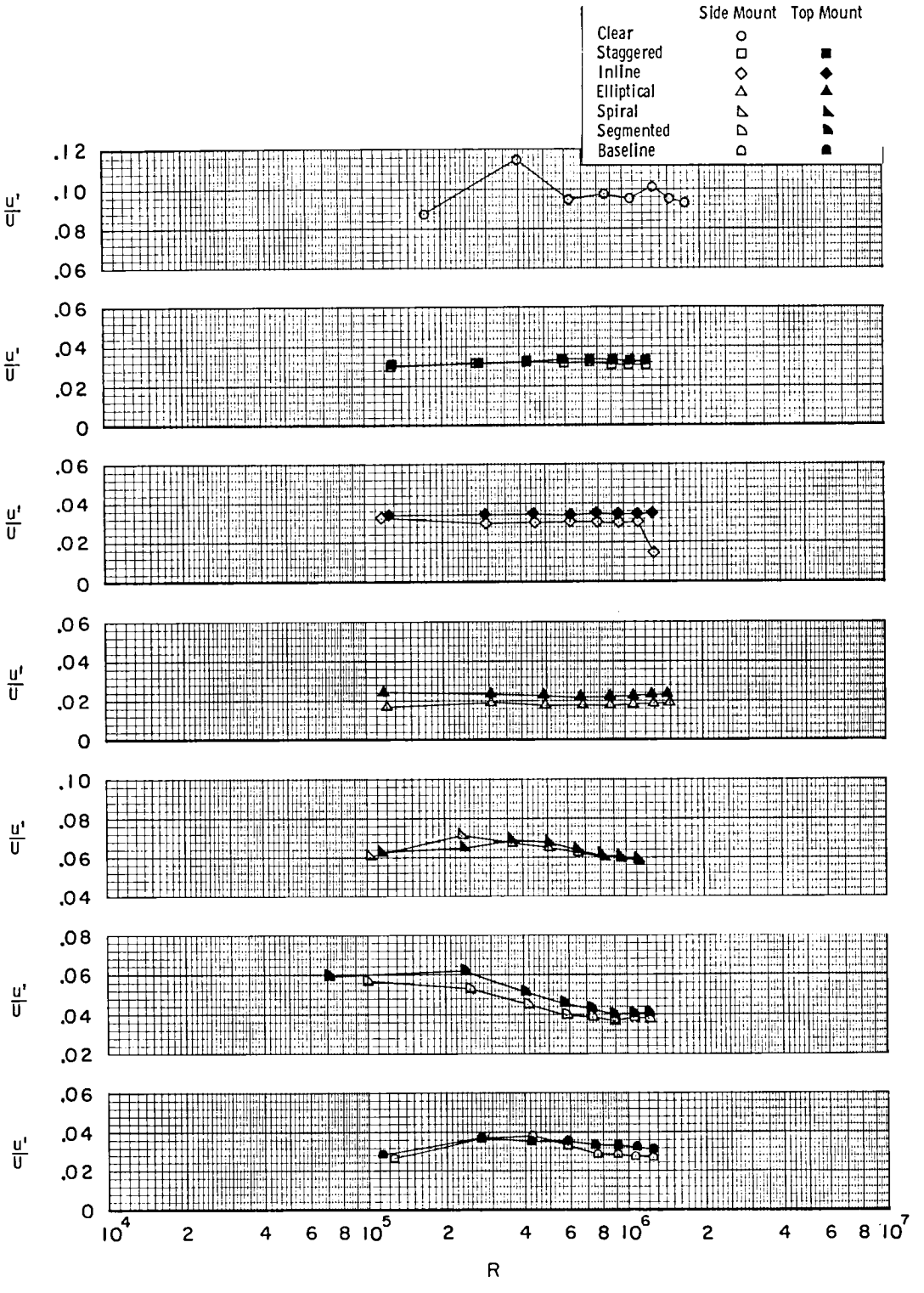

Figure 24.- Homogeneity of longitudinal turbulence with 45° oblique flow parallel to fins of cooling-coil configurations.

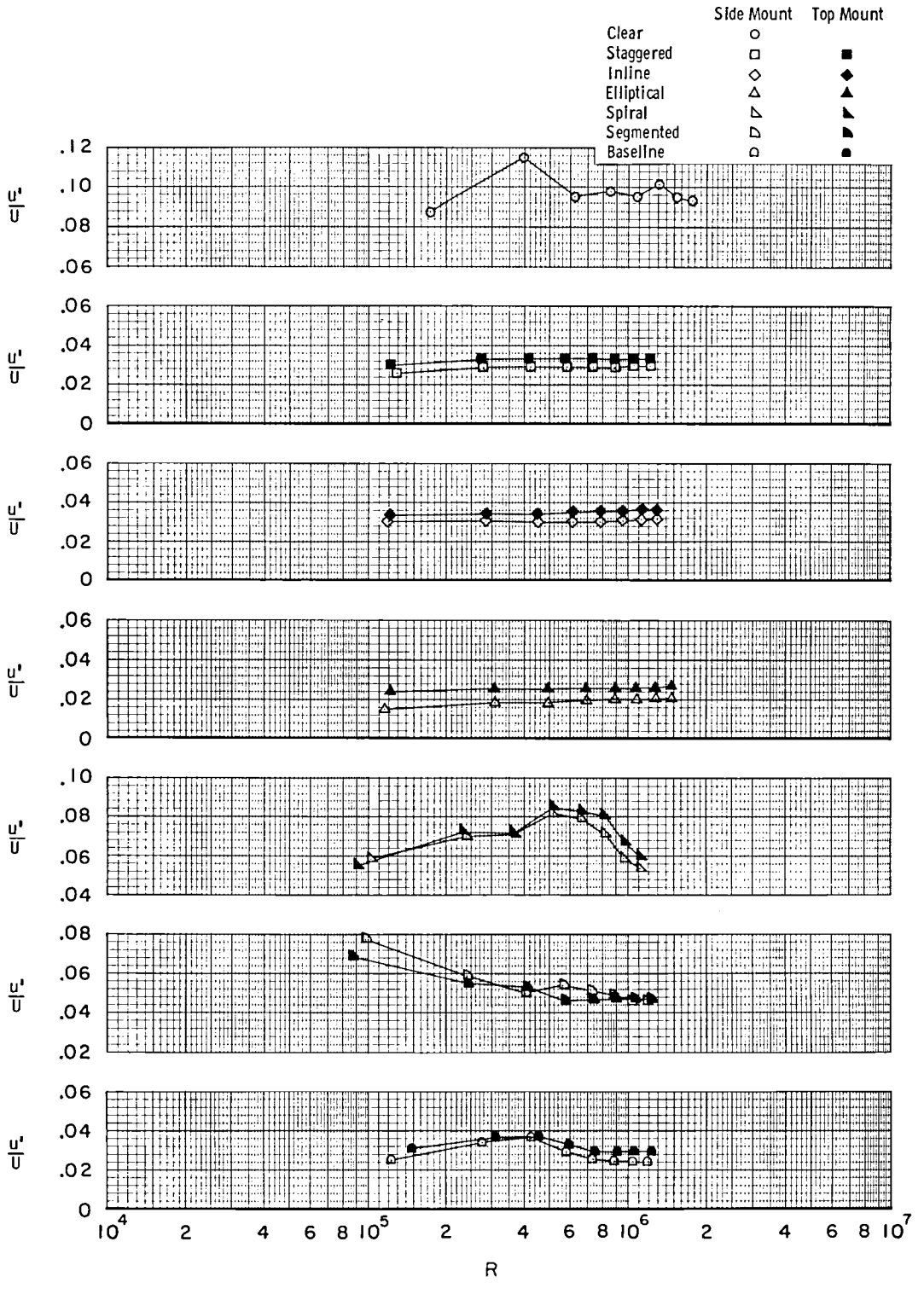

Figure 25.- Homogeneity of longitudinal turbulence with 45° oblique flow parallel to tube axis of cooling-coil configurations.

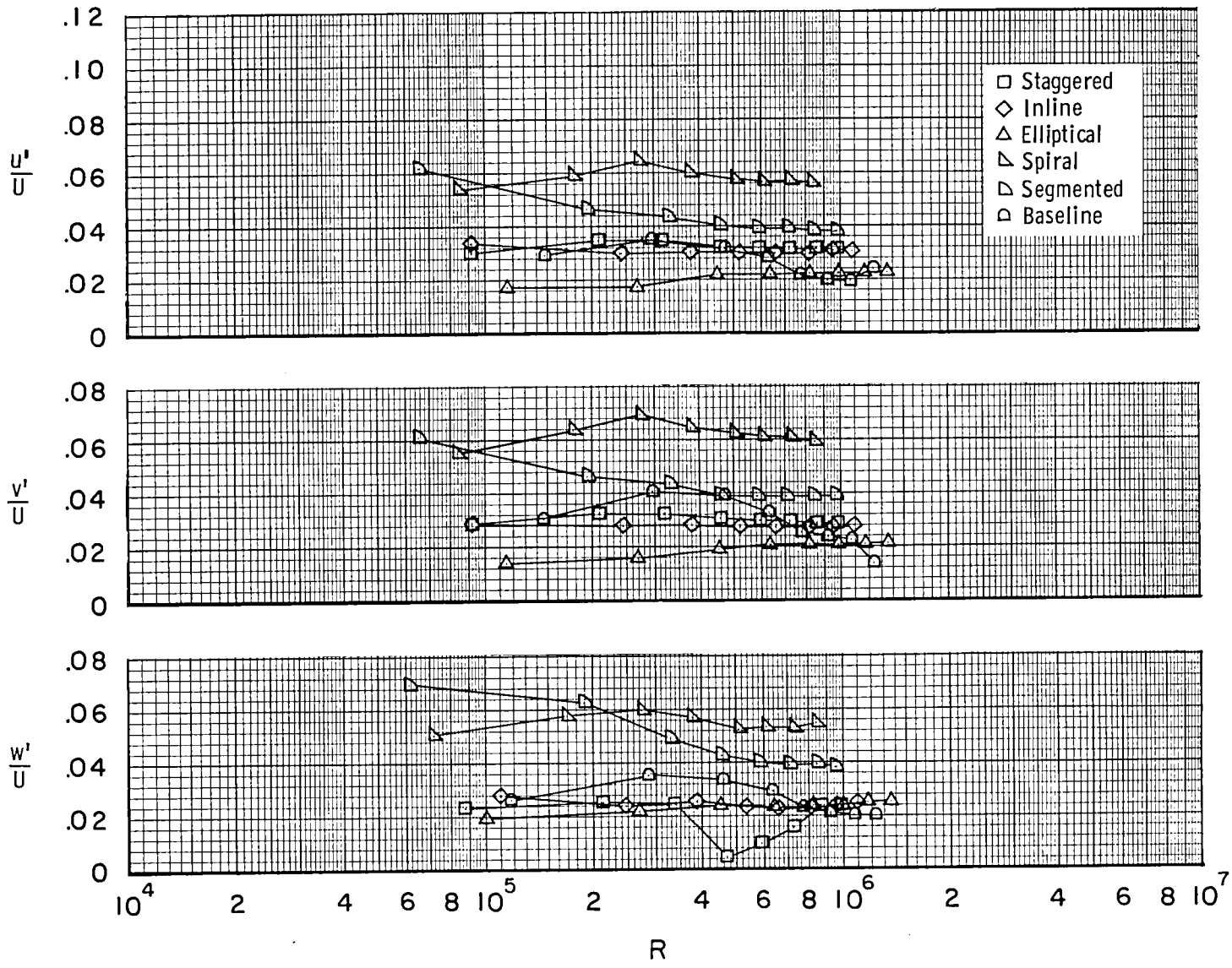

Figure 26.- Relative turbulence levels of cooling-coil configurations in normal flow.

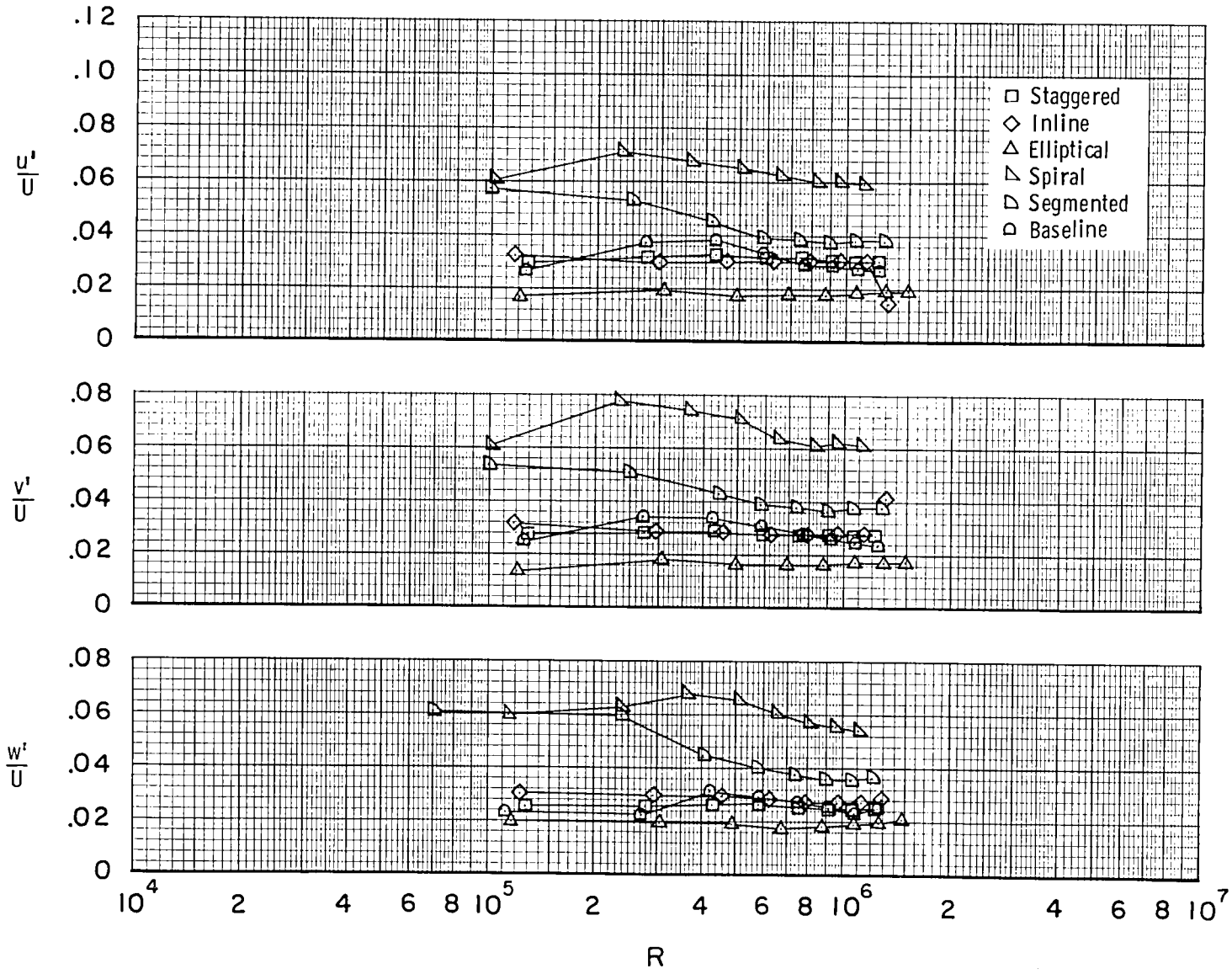

Figure 27.- Relative turbulence levels of cooling-coil configurations in 45° oblique flow parallel to fins.

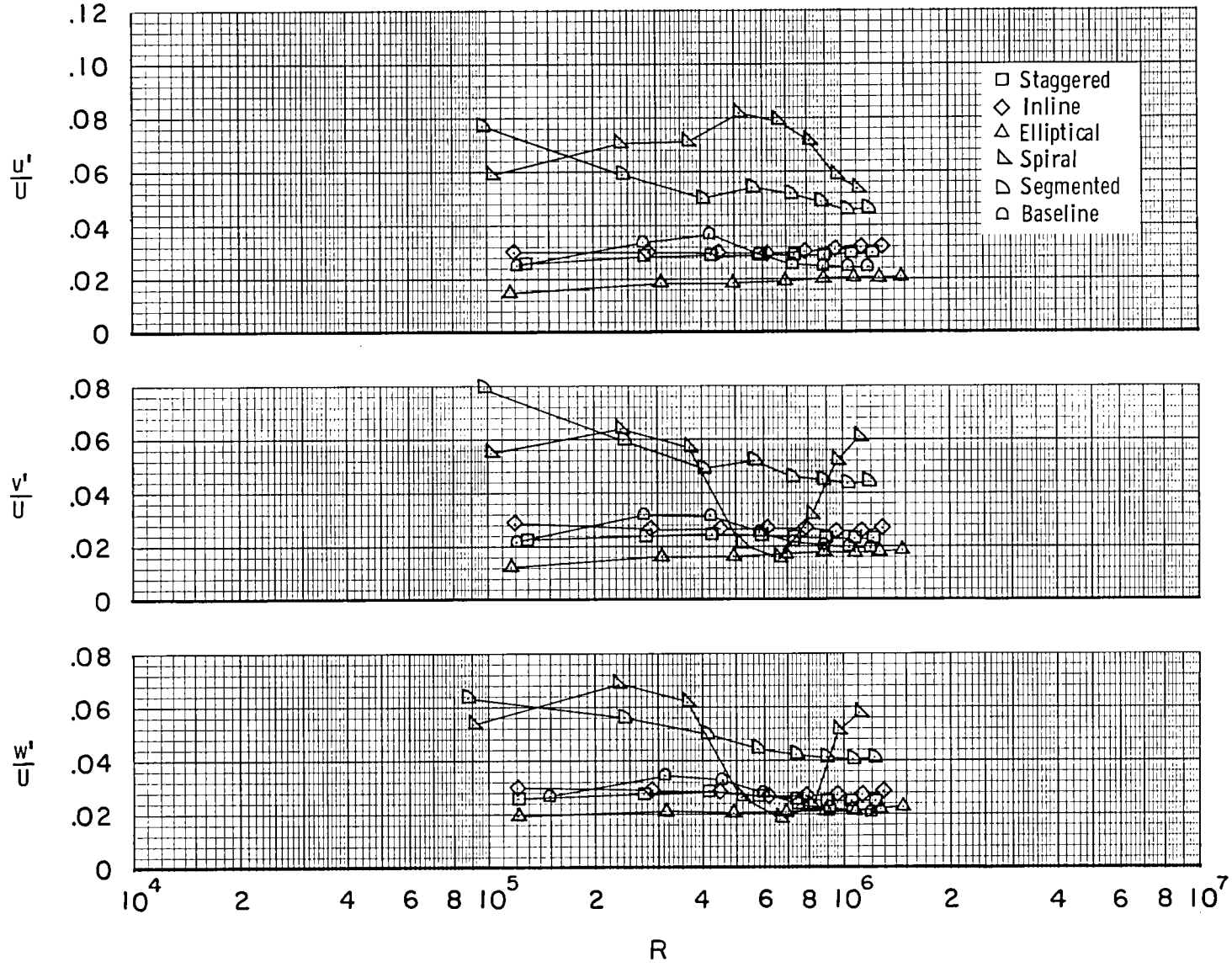

Figure 28.- Relative turbulence levels of cooling-coil configurations in 45° oblique flow parallel to tube axis.

1. Report No.	2. Government Accession No.	3. Recipient's Catalog No.
NASA TM-80188		

4. Title and Subtitle	5. Report Date
AERODYNAMIC CHARACTERISTICS AT LOW REYNOLDS NUMBERS OF SEVERAL HEAT-EXCHANGER CONFIGURATIONS FOR WIND-TUNNEL USE	December 1979
	6. Performing Organization Code

7. Author(s)	8. Performing Organization Report No.
William G. Johnson, Jr., and William B. Igoe	L-13307
	10. Work Unit No. 505-31-63-01

9. Performing Organization Name and Address	11. Contract or Grant No.
NASA Langley Research Center Hampton, VA 23665	

12. Sponsoring Agency Name and Address	13. Type of Report and Period Covered
National Aeronautics and Space Administration Washington, DC 20546	Technical Memorandum
	14. Sponsoring Agency Code

15. Supplementary Notes

16. Abstract

In response to design requirements of the National Transonic Facility, aerodynamic tests were conducted to determine the pressure-drop, flow-uniformity, and turbulence characteristics of various heat-exchanger configurations as a function of Reynolds number. Data were obtained in air with an indraft flow apparatus operated at ambient temperature and pressure. The unit Reynolds number of the tests varied from about 0.06×10^6 to about 1.3×10^6 per meter. The test models were designed to represent segments of full-scale tube bundles and included bundles of round tubes with plate fins in both staggered and inline tube arrays, round tubes with spiral fins, elliptical tubes with plate fins, and an inline grouping of tubes with segmented fins.

17. Key Words (Suggested by Author(s))	18. Distribution Statement
Heat-exchangers Finned tubes Cooling coils	Unclassified - Unlimited Subject Category 34

19. Security Classif. (of this report)	20. Security Classif. (of this page)	21. No. of Pages	22. Price*
Unclassified	Unclassified	51	$5.25

* For sale by the National Technical Information Service, Springfield, Virginia 22161

NASA-Langley, 1979

National Aeronautics and
Space Administration

Washington, D.C.
20546

Official Business
Penalty for Private Use, $300

SPECIAL FOURTH CLASS MAIL
BOOK

Postage and Fees Paid
National Aeronautics and
Space Administration
NASA-451

NASA

POSTMASTER: If Undeliverable (Section 158 Postal Manual) Do Not Return